Palaeogeography, Palaeoclimatology, Palaeoecology 441 (2016) 137–151

Contents lists available at ScienceDirect

Palaeogeography, Palaeoclimatology, Palaeoecology

journal homepage: www.elsevier.com/locate/palaeo

Upheavals during the Late Maastrichtian: Volcanism, climate and faunal events preceding the end-Cretaceous mass extinction

Gerta Keller *, Jahnavi Punekar, Paula Mateo

Department of Geosciences, Princeton University, Princeton, NJ 08450, USA

ARTICLE INFO

Article history:
Received 8 April 2015
Received in revised form 4 June 2015
Accepted 24 June 2015
Available online 2 July 2015

Keywords:
Late Maastrichtian climate
Planktic foraminifera
High-stress environments
Deccan volcanism
KTB mass extinction

ABSTRACT

The late Maastrichtian was a time of major climate, evolution and extinction extremes. Rapid climate warming of 2–3 °C in intermediate waters between 69.5 and 68 Ma (top C31r to base C30n) accompanied maximum evolutionary diversification (43% increase, zone CF5 to low CF4) in planktic foraminiferal history, followed immediately by a cluster of extinctions. During the last 250 ky of the Maastrichtian (C29r, zones CF2–CF1), rapid warming of 4 °C in intermediate waters and 8 °C on land resulted in high-stress environments ending in the mass extinction. The end-Cretaceous mass extinction is recorded in sediments between massive Deccan lava flows in India and attributed to SO_2 and CO_2 outgassing leading to ocean acidification. The early late Maastrichtian climate and faunal upheavals are not well known.

Here we document the faunal similarities of both events from the Indian Ocean through the Tethys and Gulf of Mexico. Results show that both extreme warm events are marked by high-stress environments characterized by decreased abundance and diversity of large specialized species and dwarfing, high abundance of low oxygen tolerant species, and disaster opportunist surface dweller *Guembelitria* blooms. The similarity in faunal response with the Deccan warming of C29r (CF2–CF1) suggests that volcanism was also responsible for the warming and faunal upheaval of the early late Maastrichtian. Major volcanic activity at this time included the onset of Deccan eruptions and Ninetyeast Ridge volcanism. The role of the Chicxulub impact appears to have been a contributing, rather than causal, factor in the mass extinction.

1. Introduction

The last five million years of the Maastrichtian experienced the coldest climate of the Cretaceous interrupted by two warm periods, major sea level fluctuations and faunal turnovers ending in the Cretaceous–Tertiary boundary (KTB also known as KPg) mass extinction (Li and Keller, 1998a,b; Li et al., 2000; Keller, 2001; Nordt et al., 2003). Planktic foraminifera responded to these environmental upheavals by dramatically reduced diversity after the late Campanian–early Maastrichtian cooling. This cooling was followed by rapid evolution and diversification reaching maximum Cretaceous diversity during the first warm period of the early late Maastrichtian (Keller, 2001). The second warm period near the end of the Maastrichtian marks the onset of the terminal decline leading to the mass extinction (Fig. 1).

South Atlantic DSDP Site 525A has excellent climate and faunal records that mirror global climate changes through the Maastrichtian and yield insights into the environmental conditions that led to the KTB mass extinction (e.g., Li and Keller, 1998a,b,c, 1999; Keller, 2001; Abramovich and Keller, 2002, 2003; Thibault and Gardin, 2006, 2007; Friedrich et al., 2009; Abramovich et al., 2010). From the late Campanian to early Maastrichtian, deep ocean waters cooled from an average of 16 °C to 10 °C and surface waters from 22 °C to 17 °C (Barrera, 1994; Barrera et al., 1997; Li and Keller, 1998a,b; MacLeod et al., 2005; Isaza-Londoño et al., 2006), and species diversity and $\delta^{13}C$ decreased to minimum values (Fig. 1) (Li and Keller, 1998a,c; Keller, 2001). During the early Maastrichtian magnetic reversal C31r climate remained cool and species diversity and $\delta^{13}C$ values gradually increased (Fig. 1) (Li and Keller, 1998a).

The first major change occurred in the upper C31r (CF6/CF5 transition of planktic foraminifera zones) with the onset of rapid climate warming of 2–3 °C continuing until the base C30n (Fig. 1) (Li and Keller, 1998a,c; Keller, 2001). This interval was accompanied by increased $\delta^{13}C$ values (interpreted as increasing primary productivity) and rapid evolutionary diversification in surface and intermediate water dwelling species reaching maxima from 10 to 20 species and 16 to 26 species, respectively (Fig. 1). Intermediate dwelling species gradually decreased with the onset of cooling in CF4 and accelerated their decrease through the latest Maastrichtian C29r rapid greenhouse warming. The surface dwellers held steady through the cool and warm temperatures. The response to the rapid warming at Site 525A is observed as reduced abundances and dwarfing of large complex specialized species and dominance of low oxygen tolerant *Heterohelix*

* Corresponding author at: Guyot Hall, Princeton University, Princeton, NJ 08544, USA. Tel.: +1 609 258 4117.
E-mail address: gkeller@princeton.edu (G. Keller).

http://dx.doi.org/10.1016/j.palaeo.2015.06.034
0031-0182/

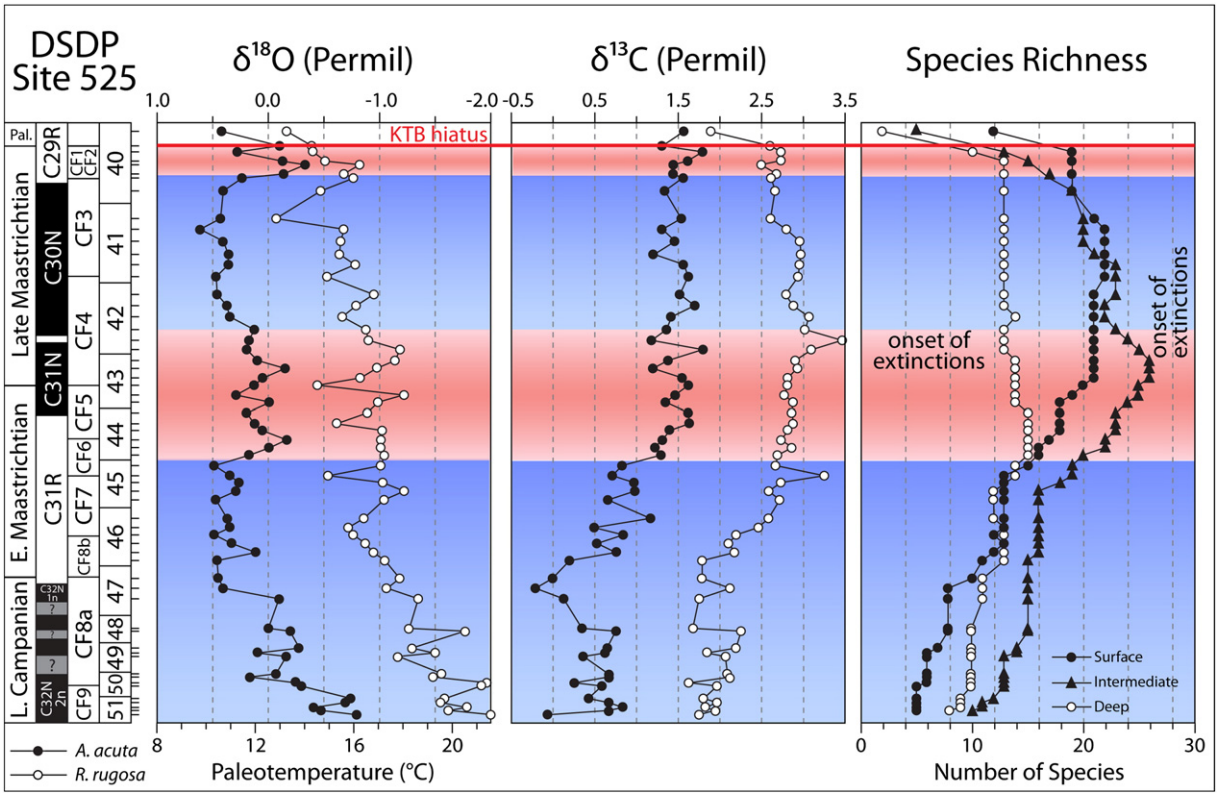

Fig. 1. Stable isotope data of planktic (*Rugoglobigerina rugosa*) and benthic (*Cibicidoides pseudoacuta*) foraminifera at DSDP Site 525A, Walvis Ridge, South Atlantic, record global climate and productivity changes from the late Campanian to the KTB mass extinction. Planktic foraminifera reveal lowest diversity by early Maastrichtian correlative with maximum cooling, highest evolutionary diversity in the early late Maastrichtian correlative with intermediate water warming and high productivity, and rapidly decreasing diversity during the latest Maastrichtian green house warming followed by the mass extinction (data from Li and Keller (1998a)).

species (Abramovich and Keller, 2003; Abramovich et al., 2003). Similar dwarfing effects combined with *Guembelitria* blooms have been observed worldwide in planktic foraminifera (Coccioni and Luciani, 2006; Keller and Abramovich, 2009). Calcareous nannofossils also strongly reflect the end-Maastrichtian warming with an increase in the relative abundance of warm-water species *Micula murus* (Thibault and Gardin, 2006, 2007, 2010; Thibault and Husson, 2016–in this issue). All but a few ecologically tolerant small planktic foraminifera rapidly went extinct at the end of the Maastrichtian coincident with another rapid greenhouse warming that is only recorded in the most complete sections immediately preceding the KTB (e.g., Elles, Tunisia, Brazos, Texas, Bottacioni, Italy, Abramovich et al., 2011; Keller et al., 2011a; Punekar et al., 2014a; Stüben et al., 2005; Thibault et al., 2015a) marking one of the five major mass extinctions in Earth's history.

For the past 35 years, the cause for the KTB mass extinction has been attributed solely to the Chicxulub impact, and Deccan volcanism, the other catastrophe being an unlikely contender. However, the impact hypothesis has remained controversial because critical evidence could not be reconciled with the Chicxulub impact (e.g., pre-mass extinction environmental changes, pre-KTB age of impact glass spherules, selective nature of extinctions and faunal turnovers (Keller, 2011, 2014; Keller et al., 2009a, 2013)). The strong belief in the impact hypothesis and its popularity as sole cause for the mass extinction left any evidence to the contrary suspect, ignored or brushed aside as result of unspecified impact-generated tsunami and earthquake effects (see Schulte et al. (2010)).

With the discovery of the KTB mass extinction in Deccan Traps of central, SE and NE India, the role of Deccan volcanism could no longer be denied (Keller et al., 2008, 2009b, 2011b, 2012; Gertsch et al., 2011). A broad cross-discipline effort is now underway to reassess the respective roles of the Chicxulub impact and Deccan volcanism (Font et al., 2011, 2014; Courtillot and Fluteau, 2014; Mussard et al., 2014). This reassessment was brought about by an improved magnetic reversal record and recognition of three phases of Deccan eruptions (Chenet et al., 2007, 2008, 2009), documentation of the mass extinction directly between lava flows (Keller et al., 2011b, 2012), and correlation with extreme rapid global warm events (reviews Keller (2014); Punekar et al. (2014a)). Recent high-precision U–Pb dating of the Deccan Trap eruptions (Schoene et al., 2015) revealed ~3000 m of lava flows erupted in just 750 ky during magnetic reversal C29r and most of the eruptions occurred in the 250 ky prior to the KTB mass extinction.

This study focuses on the late Maastrichtian environmental upheavals that encompass major global warm events, faunal turnovers and the KTB mass extinction. The database consists of quantitative planktic foraminiferal analysis from which the environmentally most sensitive species populations were chosen as indicators measuring biotic stress (e.g., large complex specialized species (globotruncanids), low oxygen tolerant species (heterohelicids) and disaster opportunists (*Guembelitria* species)). The primary objective is to document and evaluate high-stress oceanic conditions and their potential links to Deccan volcanism known from magnetic reversals C30n (and possibly upper C31n) and C29r during the late Maastrichtian (Chenet et al., 2008) and late Maastrichtian Ninetyeast Ridge volcanism (Keller, 2003, 2005; Tantawy et al., 2009). For this study we chose Madagascar, Ninetyeast Ridge, Israel and Egypt to illustrate high-stress faunas relatively close to the paleolatitude of India and compare these with records from India, South Atlantic Site 525A and Texas (Fig. 2). We assume that such a global reach indicates global environmental changes triggered by catastrophic events – Deccan and Ninetyeast Ridge volcanism. The potential role of the Chicxulub impact is discussed within this context.

2. Recent advances in Deccan volcanism

Recent studies of the Deccan Volcanic Province (DVP) in India (Fig. 3A, B) have significantly advanced our understanding of the nature

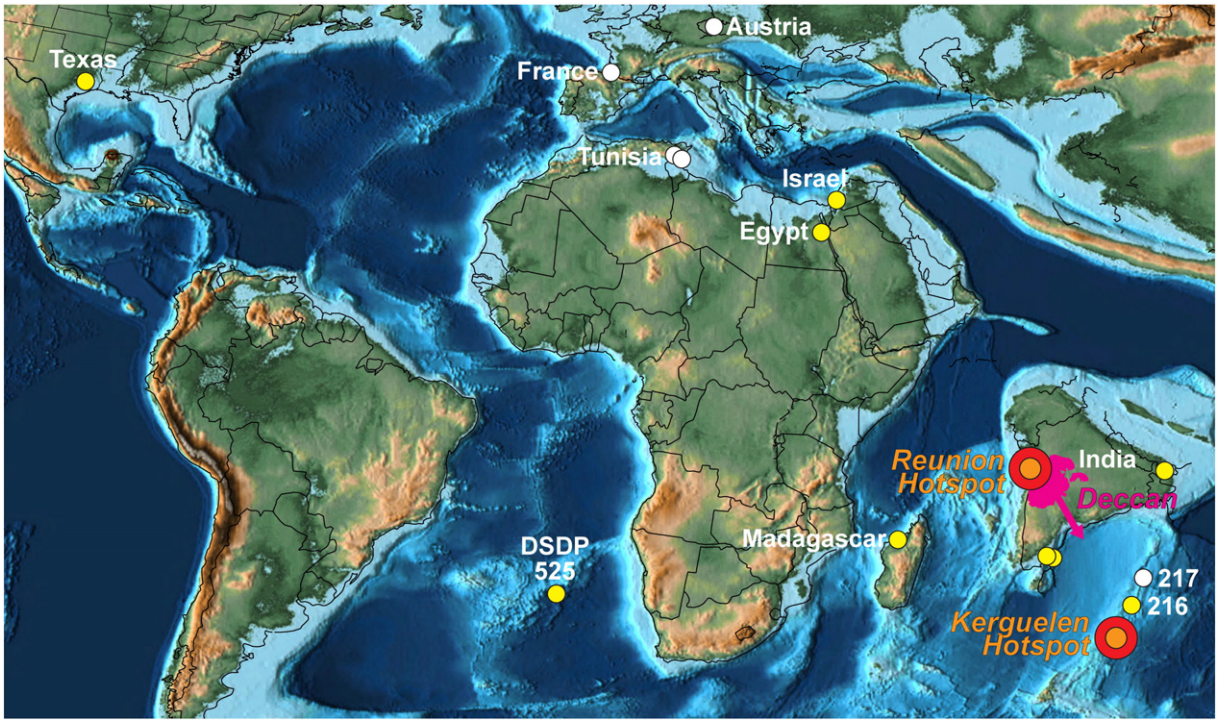

Fig. 2. Paleomap (66 Ma) of the Tethys and southern oceans with localities of Maastrichtian and KTB sections analyzed, the Reunion and Kerguelen Hotspots and Deccan volcanism. Yellow dots mark localities discussed in this study. Paleomap from Scotese (2013) showing paleogeography (mountains, land, shallow seas and deep oceans).

and tempo of these eruptions to the point where Deccan volcanism has become a serious contender in the KTB mass extinction among scientists across disciplines (Font et al., 2011, 2014; Courtillot and Fluteau, 2014; Keller, 2014; Mussard et al., 2014; Richards et al., 2015; Schoene et al., 2015). Major advances include: (1) systematic analysis of magnetic reversals and $^{40}Ar/^{39}Ar$ dating that identified three phases (phase-1, 2, and 3) of volcanic eruptions with phase-2 accounting for ~80% of the total volume (Fig. 3C,D) (Chenet et al., 2007, 2008, 2009). (2) Documentation of the earliest Danian evolution of planktic foraminifera in the aftermath of the mass extinction in intertrappean sediments between phase-2 and phase-3 lava flows in southeastern (Rajahmundry) and central India (Jhilmili) (Keller et al., 2008, 2009b) recognized as the longest lava flows on Earth (Self et al., 2008). (3) Discovery of the mass extinction in intertrappean sediments of the longest four lava flows of phase-2 in the Krishna-Godavari Basin of SE India (Keller et al., 2011b, 2012). And (4) high-precision U–Pb dating of lava flows (Schoene et al., 2015).

Deccan volcanism occurred in three short phases (Fig. 3C) with the oldest phase-1 spanning from upper C31n to middle C30n with a mean age of 67.5 ± 0.6 Ma (Chenet et al., 2007). Recently, phase-1 basaltic lava flows from the Malwa Plateau and Mandla area in central India were dated at 67.12 ± 0.44 Ma based on $^{40}Ar/^{39}Ar$ ages (Fig. 3B) (Schöbel et al., 2014). Little is known of the volume, tempo and aerial extent of phase-1 volcanism and its potential environmental consequences. No volcanic eruptions are known between 67.12 ± 0.44 Ma and 66.25 Ma, marking this as a period of volcanic quiescence.

The main phase of Deccan eruptions, phase-2, began near the base of C29r and is (U–Pb) dated at 66.288 ± 0.027 Ma and ended 750 ky later at the top of C29r dated at 65.552 ± 0.026 (Fig. 3D) (Schoene et al., 2015). A total of ~3000 m of lava flows accumulated during this time in the Western Ghats of the Deccan volcanic province (DVP, Fig. 3A,B). The stratigraphic location of the KTB in these 3000 m of lava flows is still unknown. Today the KTB is placed at 66 Ma based on $^{40}Ar/^{39}Ar$ dating of sanidine in bentonites of the Hell Creek area of Montana that yielded an age of 66.043 ± 0.086 Ma (Renne et al., 2013). This means that Deccan phase-2 began 250 ky before the KTB mass extinction. Judging from the thick single lava flows up to 100 m thick, the rate and tempo of lava eruptions were very high during these 250 ky, though the actual chronology awaits further U–Pb dating.

The KTB was first documented in Rajahmundry, SE India, at the top of four lava flows of phase-2 (also known as lower traps in this area) believed to be the world's longest lava flows extending from the Western Ghats to the Bay of Bengal (Fig. 3B) (Keller et al., 2008; Self et al., 2008). Subsequently, the KTB was also identified in central India (Keller et al., 2009b), NE India about 800 km from the DVP (Gertsch et al., 2011). In SE India the mass extinction was documented in intertrappean sediments between the four longest lava flows in deep wells drilled by India's Oil and Natural Gas Corporation (ONGC) in the Krishna-Godavari Basin (Keller et al., 2011b, 2012). Rapid global warming of 3–4 °C in the oceans and 8 °C on land during the latest Maastrichtian prior to the KTB mass extinction has been linked to Deccan phase-2 (Li and Keller, 1998b,c; Wilf et al., 2003; Thibault and Gardin, 2006, 2007; Keller et al., 2012; Keller, 2014; Punekar et al., 2014a).

The final phase-3 of volcanism began in the early Danian C29n with a U–Pb date of 65.545 ± 0.026 Ma (Schoene et al., 2015). This volcanic event is linked to the global warm event DanC2 (Quillévéré et al., 2008) and marks the end of the high-stress conditions for planktic foraminifera after the mass extinction. The global extent of high-stress environments and *Guembelitria* blooms was reviewed in Punekar et al. (2014a) and will not be considered in this paper.

3. Biostratigraphy

The high-resolution biostratigraphic zonal scheme for the Maastrichtian, originally developed by Li and Keller (1998a,c) based on DSDP Site 525A and Tunisian sites, was applied in this study as well as in all earlier published reports from which data was culled (Fig. 4). This zonal scheme has been successfully applied on a global basis particularly for low and middle latitudes. Calcareous nannofossil biozones of Burnett (1998) are shown for comparison. Also shown are

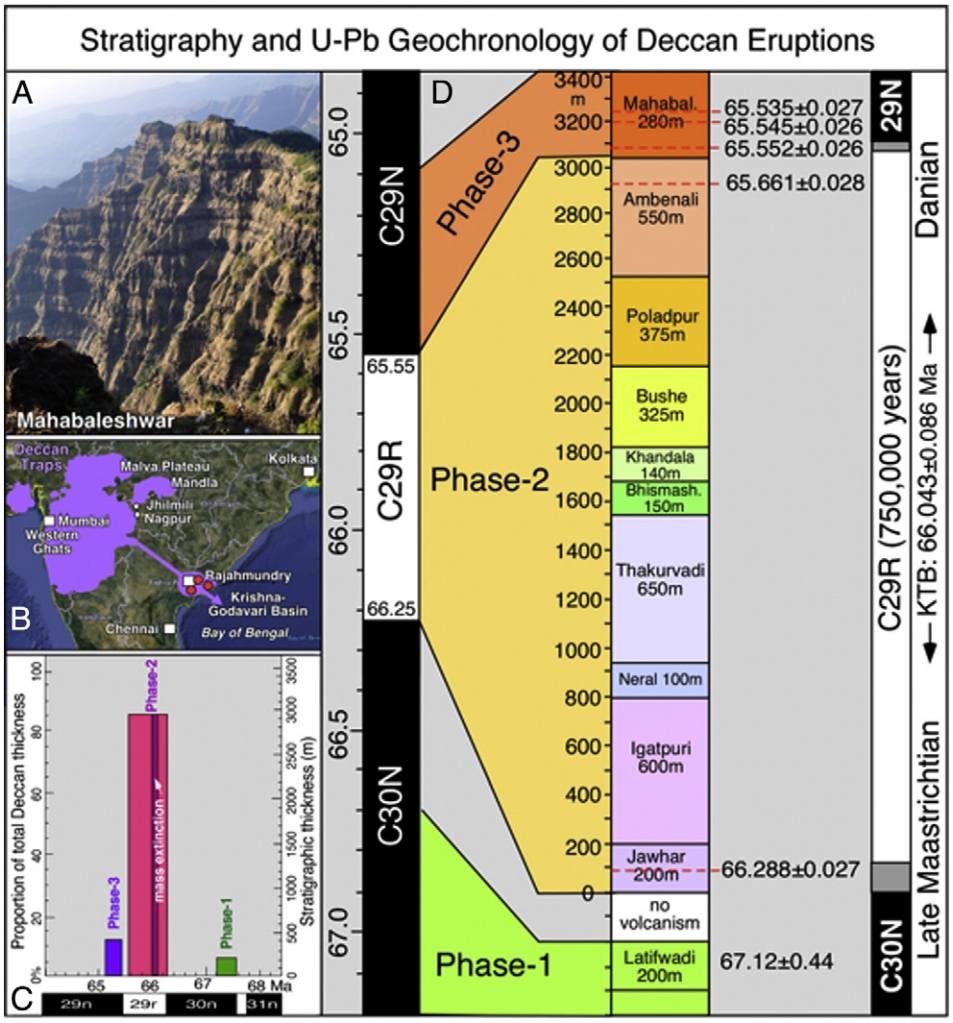

Fig. 3. Geography and stratigraphy of the Deccan Traps: (A) Deccan Traps near Mahalabeshwar, Western Ghats. (B) Geography of India showing the current extent of Deccan volcanic rocks (purple) with longest lava flows to Rajahmundry and Krishna-Godavari Basin. (C) Ages of the three phases of Deccan volcanism and estimated lava eruptions by percent of total volume. (D) Composite stratigraphic section of the Deccan Traps in the Western Ghats, with approximate formation thicknesses (Chenet et al., 2007, 2008). Paleomagnetic time scale based on the Deccan Traps is on the right with gray areas corresponding to uncertainty in magnetic reversals. The location of the KTB is still unknown in the Western Ghats. Absolute ages based on U–Pb geochronology (Schoene et al., 2015). Paleomagnetic time scale to the left (Husson et al., 2011; Schoene et al., 2015) shows the approximate duration of Deccan eruptions in each of the three phases.

cool and warm intervals based on stable isotopes of Site 525A, Deccan eruption phases, sea level events (Haq, 2014) and common hiatuses (Li and Keller, 1998a, 1999; Li et al., 2000; Adatte et al., 2002).

First and last appearances of species ideally mark evolution and extinction events. Realistically, first appearances are influenced by migration of species into formerly inhospitable environments during global warming and restricted geographic ranges during cooling. For many species this migration results in diachronous species ranges across latitudes and absence of tropical index species in higher latitudes. Despite these inherent problems, key index species used for zone identification and age dating are generally reliable. They have been tested over wide regions and include *Gansserina gansseri*, *Racemiguembelina fructicosa*, *Pseudoguembelina hariaensis*, *Contusotruncana contusa*, and *Plummerita hantkeninoides* (Fig. 4).

However, Gardin et al. (2012) concluded that Li and Keller's (1998a, c); Li et al. (1999) zonal scheme was not applicable except for CF1. The problem lies in their use of thin sections, rather than washed residues to determine the biostratigraphy (except zone CF1), which is always problematic for identifying true first and last appearances of species because of the limited faunal aspect in thin sections. In contrast, washed residue analysis provides tens of thousands of specimens from which the commonly rare first and last species appearances can be recorded. Coccioni and Premoli Silva (2015) realized this problem and based on washed residues determined a sequence of species first and last appearances that are substantially similar to Li and Keller (1998a, c) and Li et al. (1999), except for the first occurrence of *A. mayaroensis*, which is known to be diachronous across latitudes, and the last occurrence of *G. linneina*.

Most species that are not used as zonal indicators have received less scrutiny. For example, a cluster of species disappeared between the top C31r and middle C30n, including *Globotruncana bulloides*, *Contusotruncana fornicata* and *Contusotruncana plummerae*, (Fig. 5). Disappearances of some of these species are reported from Egypt (Keller, 2002; Punekar et al., 2014b), Israel (Abramovich et al., 1998, 2010), Tunisia (Li and Keller, 1998c; Li et al., 1999; Abramovich and Keller, 2002), Gubbio area (Coccioni and Premoli Silva, 2015), South Atlantic Sites 21 and 525A (Li and Keller, 1998a,c), Madagascar (Abramovich et al., 2002) and the Cauvery Basin, SE India (Fig. 5). Last appearances vary mainly due to rare specimens at the end of their stratigraphic range, potential diachronous occurrences across latitudes and short hiatuses that may or may not be recognized in routine biostratigraphy.

For example, the CF4/CF3 transition is commonly marked by a hiatus (Figs. 4, 5) due to a major sea level fall and sequence boundary at 66.8 Ma (Haq, 2014). Other hiatuses are common at the CF4/CF5 and

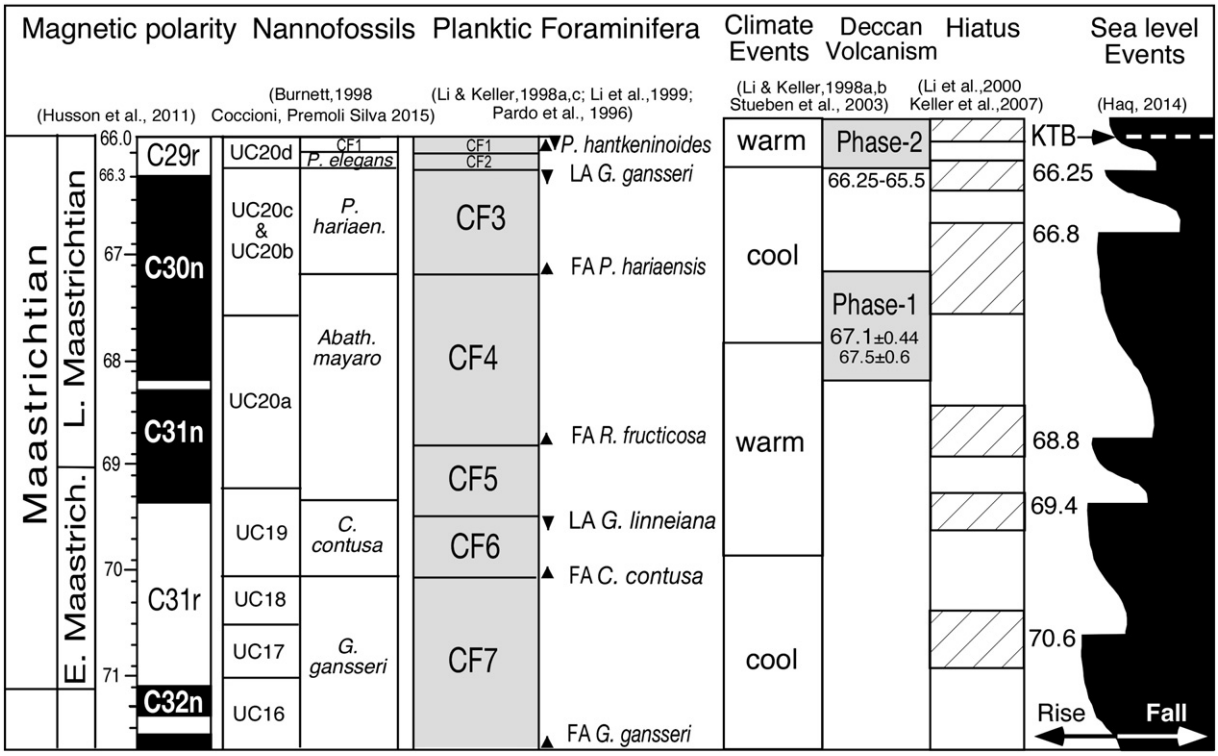

Fig. 4. Maastrichtian stratigraphy and oceanographic events applied in this study and comparison with Gubbio area sections (Coccioni and Premoli Silva, 2015). Planktic foraminiferal biozonation based on Li and Keller (1998a,c) and Pardo et al. (1996). Deccan phases based on Chenet et al. (2007, 2008), Keller et al. (2011b) and Schoene et al. (2015). Other sources of data given in the figure.

CF5/CF6 transitions due to sea level falls at 68.8 Ma and 69.4 Ma respectively (Fig. 4). Although these hiatuses complicate evaluation of the complete species ranges, the disappearances of zone CF4 taxa occurred during the end of climate warming coupled with a rising sea level correlative with the upper C31n to base C30n interval and marking a critical time interval in the early late Maastrichtian when evolutionary diversification ended and extinctions began (Keller, 2001) (Fig. 1). In the five sites examined, the biostratigraphic disappearances of these species mark the lower part of zone CF4, although the exact interval cannot be determined (Fig. 5).

3.1. Madagascar

During the late Maastrichtian, Madagascar was located at the same paleolatitude as India and South Atlantic Site 525A (Fig. 2). A late Maastrichtian to early Paleocene sequence from the Mahajanga Basin of Madagascar was chosen to evaluate the environmental effects of Deccan volcanism in India as a result of the Reunion hotspot (Fig. 2). The Amboanio section is located about 28 km to the south of the city of Mahajanga in the northern end of Bombetoka Bay. The Maastrichtian consists of marls and marly limestone rich in macrofossils and well preserved diverse planktic foraminiferal assemblages deposited in a middle neritic environment that shallowed to inner neritic depths and became subaerial by the KTB (Abramovich et al., 2002).

The late Maastrichtian at Amboanio and a second shallower section analyzed at Berivotra (located 80 km southeast of Mahajanga) are incomplete (Abramovich et al., 2002). At Amboanio, the 5.8 m at the base of the section mark a part of zone CF4, an interval dominated by relatively steady populations of *Guembelitria* (*G. cretacea* and *G. dammula*, 50–60%) and common globotruncanids (total 20–25%). Biserial taxa are dominated by *Heterohelix globulosa* (25–40%) and *Heterohelix planata* (30–40% decreasing to 10%) but only few *Heterohelix (Spiroplecta) navarroensis* and rare *Heterohelix labellosa* and *Pseudoguembelina palpebra* (Fig. 6). Abrupt population changes and onset of *Pseudoguembelina hariaensis*, the index species for zone CF3, and termination of *R. plummerae* and *G. ventricosa* mark a major hiatus at the CF4/CF3 interval. Another hiatus at Berivotra juxtaposes CF4/CF6 and terminates *Globotruncana linneiana*, *G. bulloides*, and *C. fornicata* (Fig. 5). Both hiatuses coincide with sea level regressions dated at 66.8 Ma and 68.8 Ma (Haq, 2014) (Fig. 4). At Berivotra, the CF5/CF4 boundary is tentatively based on a single occurrence of the index species *R. fructicosa*, whereas *G. bulloides*, *C. plummerae*, *G. linneiana* and *Gansserina wiedenmayeri* disappear simultaneously 3 m below suggesting a hiatus (Abramovich et al., 2002).

In zone CF3 above the hiatus at Amboanio, globotruncanids drop >30% to 3–12% decreasing to near zero in zones CF1–CF2, except for the last sample, which is biased by preferential preservation of keeled species and dissolution of others (Abramovich et al., 2002). *Guembelitria* populations drop from >45% to 5–15% (6–7.9 m) in zone CF3, and sharply increase in the top meter of brown marl to 30% (single point peak) and to 40% in CF2–CF1 (Fig. 6). In contrast, *H. globulosa* thrived (40%) in CF3 through CF2–CF1, *H. planata* reached 40% in zone CF3 decreasing to 10% in CF2–CF1. No foraminifera are present in the 10 cm thick volcanic ash layer at the top of the Maastrichtian.

An unconformity marks the KTB with an erosion surface and karstification overlain by a 1.2 m thick bioclastic grainstone with no microfossils and rich in volcanic ash. The KTB hiatus is estimated to span from the CF2–CF1 interval through early Danian zone P1c (Abramovich et al., 2002). Hiatuses of similar magnitude are observed in the Cauvery Basin of India (Fig. 5), Ninetyeast Ridge Site 216, South Atlantic Sites 525A, 738, 690 and Argentina (Keller, 1993, 2003; Li and Keller, 1998a; Keller et al., 2007). Erosion across the KTB is likely a function of sea level falls in the early Danian (MacLeod and Keller, 1991; Adatte et al., 2002; Haq, 2014) in relatively shallow shelf areas and intensified circulation in deeper waters. The latest Maastrichtian is therefore incomplete in Madagascar. Nevertheless, some of the characteristic *Guembelitria* blooms below the KTB hiatus are present albeit with

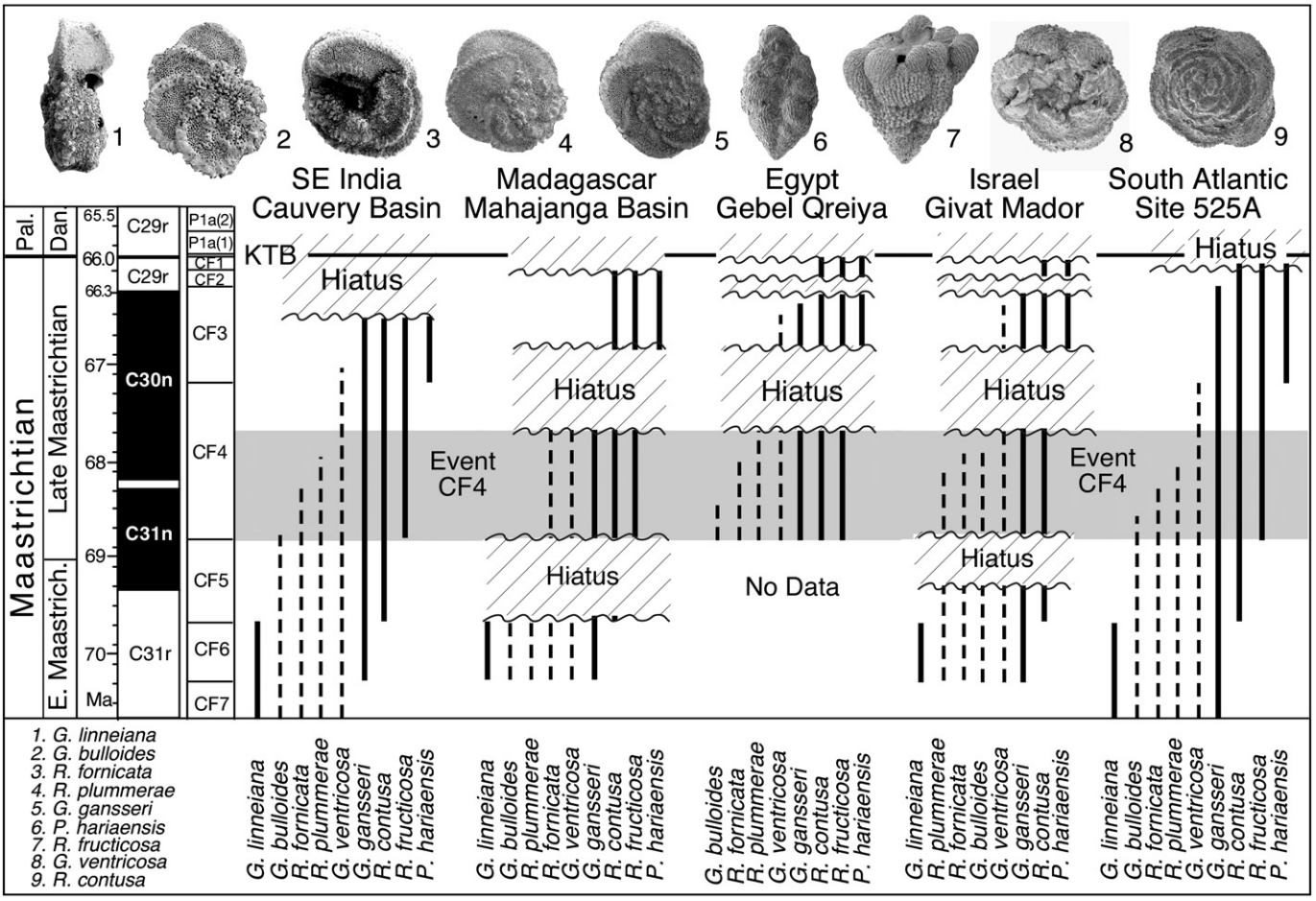

Fig. 5. Event stratigraphy of selected Campanian holdover species and index taxa that evolved during the Maastrichtian with SEM illustrations. Dashed lines mark sequential extinctions of Campanian species in the lower part of zone CF4 (*Contusotruncana contusa*, *Racemieguembelina fructicosa*, *Pseudoguembelina hariaensis*) correlative with the end of the early late Maastrichtian warming. Hiatuses are frequently observed across the KTB, CF3/CF2 and CF4/CF3, correlative with sea level falls (see Fig. 4). Data from: India, Madagascar (Abramovich et al., 2002), Egypt (Keller, 2002; Punekar et al., 2014b), Israel (Abramovich et al., 1998, 2010), Site 525A (Li and Keller, 1998a).

lower abundance. The only evidence of volcanic input in the section is observed in the ash layer below the KTB hiatus, which may correspond to Deccan phase-2 that spans C29r.

Oxygen isotope values provide some clues to relative temperature changes in Madagascar. In zone CF4 relatively steady warm surface and bottom water temperatures prevailed at Amboanio with a 1.5‰ surface-to-deep gradient (Fig. 6). In the top 1.6 m below the CF4/CF3 hiatus, increased $\delta^{18}O$ values and a decreased surface-to-deep gradient mark cooler temperatures (Abramovich et al., 2002). Above the hiatus in zone CF3, a steady warm climate is indicated in surface waters but increasingly warmer bottom water temperatures suggest a shallower environment possibly linked to the sea level fall at 66.8 Ma (Haq, 2014) and/or uplift associated with volcanism. This apparent warming in Madagascar correlates with maximum global cooling, a sea level fall and erosion at or near the C30n/C29r reversal and CF3/CF2 boundary (Li et al., 1999; Abramovich et al., 2002; Adatte et al., 2002; Keller et al., 2002). Erratic $\delta^{18}O$ values in zones CF2–CF1 reflect dissolution, post-depositional alteration and subaerial exposure.

Carbon isotope values in zone CF4 average 1.2‰ and gradually decrease towards the top of CF4 reaching the lowest values at the CF4/CF3 hiatus (Fig. 6). The near absence of a surface-to-deep gradient reflects deposition in the photic zone. Above the hiatus $\delta^{13}C$ values average 0.8‰ in both surface and bottom waters indicating a shallower depositional environment.

3.2. Ninetyeast Ridge DSDP Site 216

Ninetyeast Ridge is a north-south basaltic volcanic chain that formed as a hotspot track by the northward migration of the Indian plate over the Kerguelen hotspot estimated between 77 and 43 Ma (Fig. 2) (e.g., Duncan, 1978, 1991; Royer et al., 1991; Pringle et al., 2008; Frey et al., 2011; Krishna et al., 2012). Based on $^{40}Ar/^{39}Ar$ step-heating and a linear north-south age progression of 118.5 km/my for the India plate, Pringle et al. (2008) estimate an age of 73 Ma for basalts at Site 216.

During the late Maastrichtian Site 216 was located at about 40°S and its passage over the Kerguelen hotspot resulted in lithospheric uplift and volcanic activity lasting about 2 my (Fig. 2). Sedimentation above basement basalt consists of volcanic vesicular ash successively followed by phosphatic and glauconitic volcanic deposits and eventually chalks as Site 216 passed beyond the influence of the hotspot volcanic activity. Planktic foraminifera and calcareous nannofossils living in this volcanically influenced environment record high-stress conditions marked by extremely low species diversity, dominant *Guembelitria* blooms (80–90%) within CF4/UC20a and common to abundant low oxygen tolerant *Heterohelix* species at times of improved conditions within CF4/UC20b-c (Fig. 7) (Keller, 2003; Tantawy et al., 2009).

In an earlier study, Keller (2003) correlated the Ninetyeast Ridge Site 216 high-stress fauna with similar assemblages in Madagascar, Israel

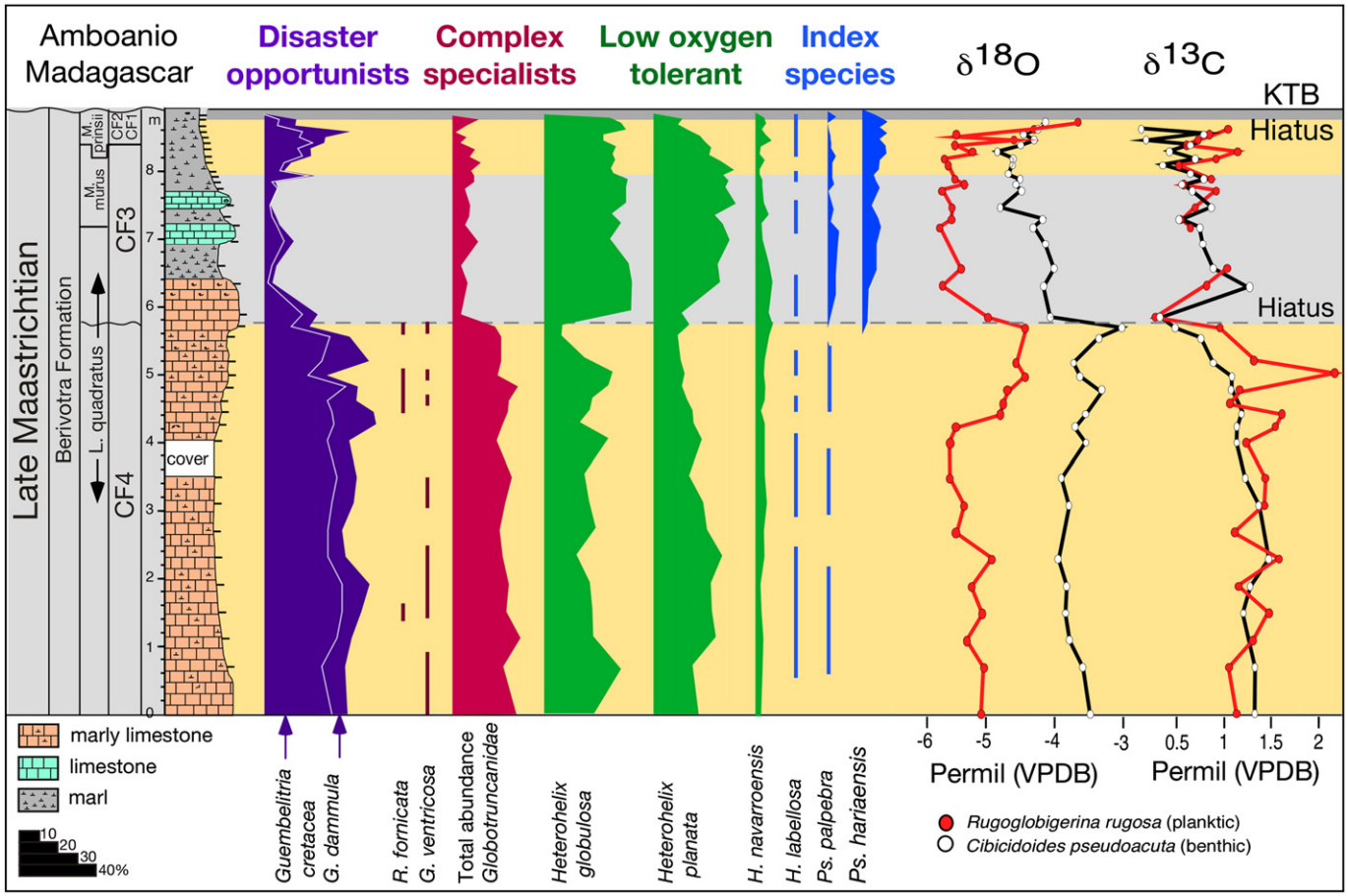

Fig. 6. Late Maastrichtian stable isotope and planktic foraminiferal stratigraphy of dominant species at Amboanio, Madagascar. Dominant species groups fall under three categories: (1) large, complex specialized species that thrived in deeper waters (thermocline) at times of warm temperatures and high water stratification. (2) Low oxygen tolerant small *Heterohelix* species that thrived in relatively high stress environments with expanded oxygen minimum zones. (3) *Guembelitria* species, known as disaster opportunists for their ability to thrive in high-stress conditions where few other species survived. Based on these groupings, the late Maastrichtian in Madagascar experienced high-stress environments in zones CF4 and CF2–CF1, two intervals correlative with Deccan phase-1 and phase-2 volcanism. Note the relatively low *Guembelitria* abundance in CF2–CF1 due to the KTB hiatus and incomplete record. (Data from Abramovich et al. (2002)).

and Egypt, attributing the stress conditions to both Ninetyeast Ridge volcanism and Deccan volcanism (phase-1). However, the timing of the volcanic interval at Site 216 remained questionable in the absence of index species for sediments older than CF2–CF1, which were attributed to zone CF3. The nannofossil study by Tantawy et al. (2009) provides improved dating with zone UC20a, correlative with planktic foraminifer zones CF5–CF4 directly overlying basement basalt. This indicates an age of ~69.5 Ma for the onset of Ninetyeast Ridge volcanism at Site 216, which correlates well with the rapid global warming beginning at the base of zone CF5 (Fig. 1).

Faunal assemblages mark extreme stress conditions with *Guembelitria* blooms dominating (80–90%) in zone UC20a and decreasing in the lower part of zone UC20b,c above (Fig. 7). The placement of the CF4/CF3 boundary is unclear due to the absence of the index species. The *Guembelitria* abundance fluctuations in the upper part mark variable stress though improving conditions with low oxygen tolerant small *Heterohelix* species replacing *Guembelitria*. Among the low oxygen tolerant species, the presence of the high latitude *Zeauvigerina waiparaensis* is notable, a species that is rare in Madagascar. More diverse foraminifer assemblages are observed as Site 216 moved away from the Kerguelen hotspot by the late Maastrichtian (C29r, zones CF2–CF1, UC20d).

3.3. Israel

Maastrichtian to early Danian sequences have been studied from the Negev (Zin valley syncline) in Israel, focusing on the KTB transition (Keller and Benjamini, 1991; Keller et al., 1991; Magaritz et al., 1992) and the late Maastrichtian (Abramovich et al., 1998, 2010; Keller, 2004). Here we review dominant species groups, *Guembelitria* blooms, some index taxa and a small cluster of disappearing Campanian holdover taxa in the late Maastrichtian. We chose Givat Mador (Abramovich et al., 1998) and Hor Hahar (Keller et al., 1991; Abramovich et al., 1998, 2010) as complimentary sections. Both are located in the Zin valley syncline and were deposited in an upper continental slope environment at a paleolatitude of about 12°N (Almogi-Labin et al., 1990; Camoin et al., 1993).

Upper Maastrichtian sediments consist of chalk, marly chalk and dark gray clayey marl. We follow Abramovich et al. (2010) for the biostratigraphy of Givat Mador, but separate CF4 and CF3 based on *Guembelitria* blooms, the extinctions of *C. plummerae* and *G. bulloides*, followed by increased abundance of Globotruncanidae, *H. globulosa*, *H. labellosa* and *Gansserina gansseri* (Fig. 8). Although all biozones are present, hiatuses are present at zonal boundaries associated with cool events, major sea level falls and erosion (Figs. 4, 5, 8).

Two *Guembelitria* bloom events are observed in dark clayey marls. The first bloom in zone CF4 reaches 50% and decreases by the middle of CF4. (Note that due to hiatuses at the base and top of CF4, the part of zone CF4 present is uncertain). The second *Guembelitria* bloom is at the top of the Maastrichtian zones CF2–CF1 and well documented worldwide (review in Punekar et al. (2014a)). At Givat Mador this bloom is relatively minor reaching only 25% and tailing off in the 3 m below the KTB. This is unusual because in complete KTB sections

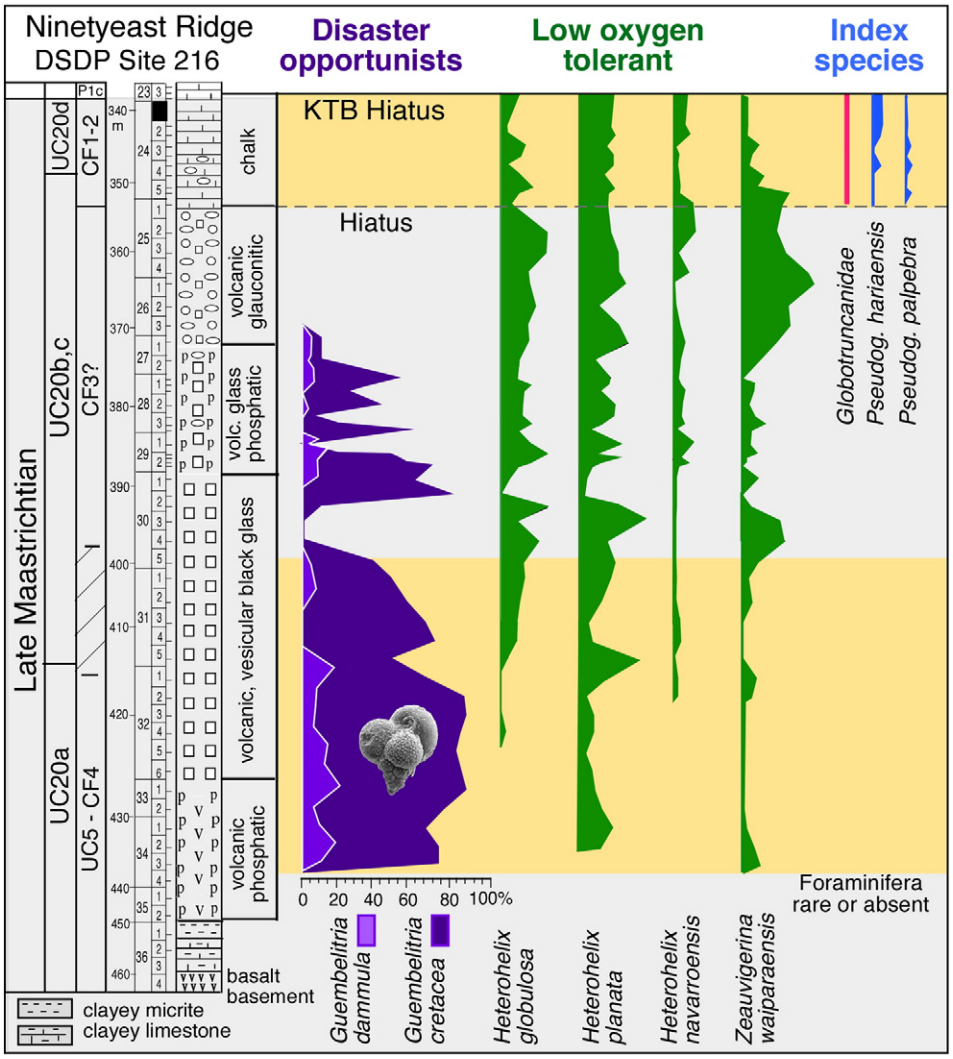

Fig. 7. Late Maastrichtian high-stress planktic foraminifer assemblages at DSDP Site 216 on Ninetyeast Ridge during volcanic eruptions (Kerguelen hotspot) beginning ~69.5 Ma coincident with rapid global warming. Maximum stress assemblages consist of 80–90% *Guembelitria* blooms and times of lower stress are dominated by low oxygen tolerant small *Heterohelix* species. (Data from Keller (2003); Tantawy et al. (2009)).

Guembelitria blooms in CF2–CF1 reach 80% or more up to the KTB mass extinction (Keller, 2002; Abramovich et al., 2011; Keller et al., 2011a; Punekar et al., 2014a). This low *Guembelitria* abundance at Givat Mador and some other Zin valley sections (Abramovich et al., 2010) is likely due to an incomplete latest Maastrichtian sediment record (note that all sections in Israel and Egypt have a KTB hiatus) and/or dwarfing in high-stress environments. The latter is frequently observed and requires analysis of the 38–63 μm size fraction, which reveals significantly higher abundances (~50–60%), though this data is not available for Givat Mador.

Large complex specialized species, primarily globotruncanids (>150 μm) average 15% with peaks of 25% in the lower part of the section up to the CF4/CF3 hiatus. Above the hiatus in the lower part of zone CF3, Globotruncanidae reach 40% and terminally decrease to extinction at the KTB, though with a peak of 15% at the CF2/CF1 boundary (Fig. 8).

Low oxygen tolerant taxa are dominated by *H. globulosa*, which reach peaks of 40–50% in the >150 μm size fraction and 60–70% in the >63 μm size fraction through the Maastrichtian with decreased abundance during the CF4 *Guembelitria* bloom. *Heterohelix planata* and *H. navarroensis* are minor components largely restricted to the lower part of the section (zone CF4, base CF3). This is unusual since both species are generally well represented or even dominant through the Maastrichtian in Egypt and *H. globulosa* and *H. planata* are equally abundant in Madagascar and common in Site 216 (Figs. 6, 7). The higher abundance of small *H. globulosa* (>63 μm) may be an artifact of grouping small biserial *H. planata* with *H. globulosa*, which was commonly done in the 1990s when this dataset was generated.

3.4. Egypt

The Gebel Qreiya section is located 50 km northeast of Quena City in the Eastern Desert. Sedimentation occurred on the stable shelf of the Asyut Basin (Said, 1962) in middle to outer neritic shelf depths and exposed to sea level fluctuations and local tectonic activity (Hendriks et al., 1987; Tantawy et al., 2001). This is one of the most complete late Maastrichtian sections in Egypt, although high-resolution lithologic and biostratigraphic analyses reveal short hiatuses largely corresponding to sea level fluctuations (Keller, 2002; Keller et al., 2002; Punekar et al., 2014b).

The upper Maastrichtian consists of monotonous gray shale with macrofossils (*Pecten farafraensis*) up to 1.8 m below the KTB where shale grades into marly shale devoid of macrofossils. About 10 cm below the KTB an undulating erosional surface truncates the marly shales. The last 10 cm of the Maastrichtian consist of burrowed marly gray shale with small macrofossils (bivalves and gastropods). The KTB

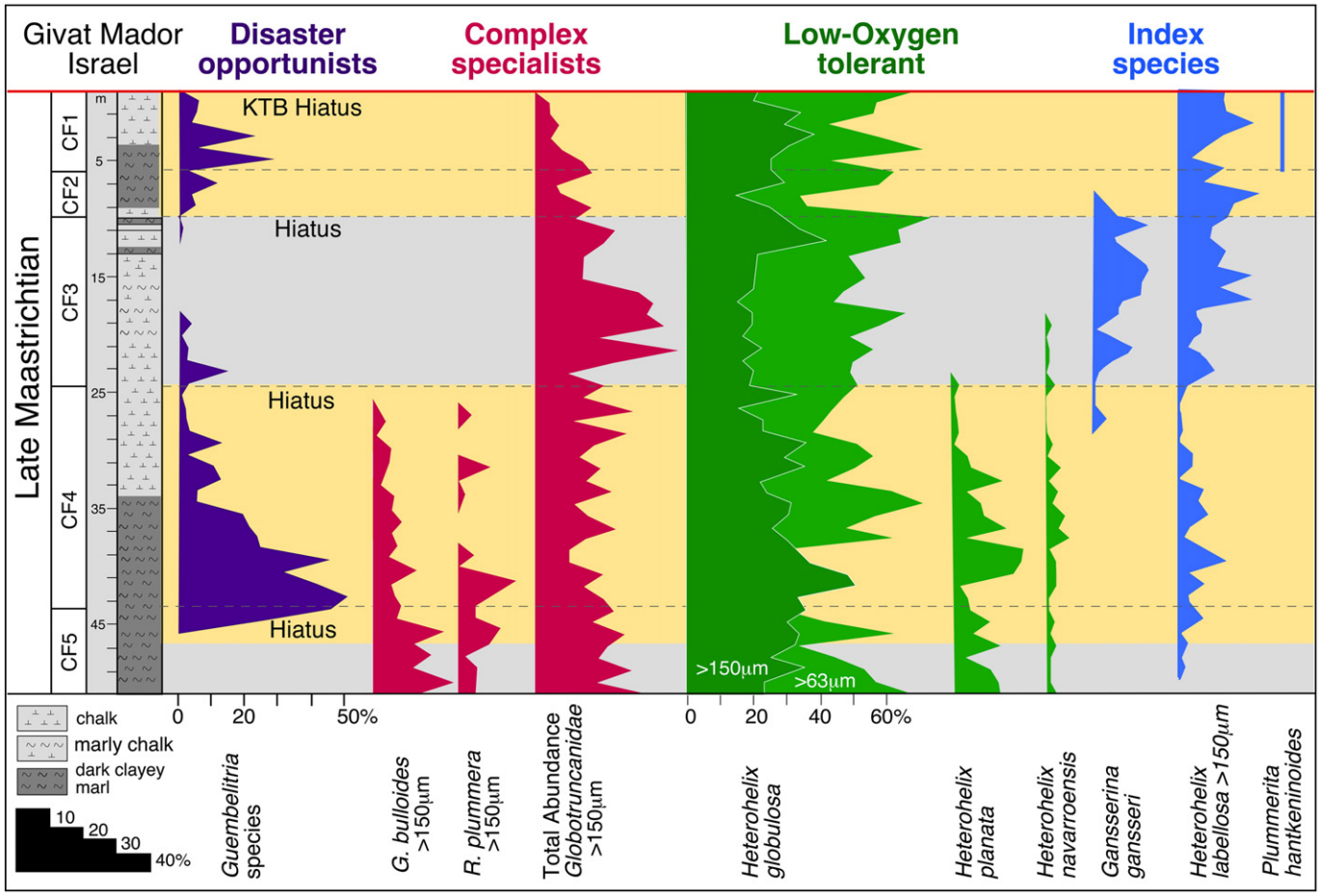

Fig. 8. Late Maastrichtian planktic foraminifer stratigraphy and selected dominant species groups marking high-stress environments at Givat Mador, Israel (data from Abramovich et al. (1998)). Two *Guembelitria* blooms mark maximum stress environments coeval with rapid global warming. Note that the relatively low blooms at the end of the Maastrichtian are due to an incomplete record and species dwarfing to sizes below the 63 µm analyzed in this datatset. Globotruncanidae terminally decline in the late Maastrichtian though with a temporary increase in the lower part of CF3. The overabundance of small (>63 µm) *Heterohelix globulosa* is likely due to inclusion of *H. planata* as commonly done in the 1990s when this dataset was generated. The disappearances of *Globotruncana bulloides* and *Contusotruncana plummerae* near the CF4/CF3 hiatus and the abundance of *Gansserina gansseri* in CF3 along with common *Heterohelix labellosa* are excellent stratigraphic markers.

is truncated by an erosion surface and overlain by a redox boundary marked by a thin red layer and dark gray clay.

Zone CF4 marks the 7 m at the base of the section, though only part of this zone was recovered (Fig. 9). A hiatus at the CF4/CF3 boundary is identified based on the disappearances of *C. fornicata*, *C. plummerae*, *C. plicata*, *G. bulloides* and *Archaeoglobigerina cretacea* as also observed in Israel and Madagascar (Abramovich et al., 1998, 2002, 2010). Dominant species abundances are variable. The disaster opportunist *Guembelitria cretacea* peaks at about 60% near the bottom and top of zone CF4 with just 13% in between (Fig. 9). Globotruncanids average as low as 5% at times of high *Guembelitria* abundance and reach two peaks of 25% and 30% in intervals of low *Guembelitria*. Similar inverse fluctuations are observed in low oxygen tolerant *Heterohelix* species (*H. globulosa*, *H. planata*, *H. navarroensis*). *Heterohelix (Spiroplecta) navarroensis* is unusually common at Qreiya though relatively few in Site 216, Madagascar or Israel (Figs. 6, 7). Note the relatively low abundance of *H. globulosa*, but high *H. planata* compared with Israel and Madagascar suggests a taxonomic problem at Givat Mador.

Zone CF3 spans the interval from 7 to 15 m, marked by the last *G. gansseri* and increased *H. labellosa* (Fig. 9). *Gansserina gansseri* is rare at Gebel Qrieya. Keller (2002) and Punekar et al. (2014b) placed the top of the last appearance of *G. gansseri* coincident with the first appearance of *P. hantkeninoides*, the index species for CF1. Re-examination of those isolated '*G. gansseri*' specimens reveal them to be *Globotruncana pettersi*, which means that zone CF2 is present.

Guembelitria cretacea blooms reach 60% in two intervals of zone CF3 corresponding to the dark organic-rich shale with macrofossils (*Pecten farafraensis*) but <10% near the base and top of the zone. Globotruncanids are generally <5% except in a single interval at the onset of the first *Guembelitria* bloom (60%), and nearly absent near the top of CF3 (Fig. 9). Low oxygen tolerant *Heterohelix* species are common but variable and tend to inversely correlate with intervals of high *Guembelitria* abundances as also observed in Israel and Madagascar.

Zone CF2 marks the interval between the last appearance of *G. gansseri* to the first appearance of *P. hantkeninoides*, which at Qreiya spans from 15 to 17.5 m. Zone CF1, identified by the range of *P. hantkeninoides* spans the top 1.8 m of the Maastrichtian (Fig. 9). *Guembelitria* blooms reach 97% in CF2. The abrupt faunal change between CF3/CF2 coincides with the 66.25 Ma sea level fall and maximum cooling at the CF3/CF2 transition. The reduced *Guembelitria* blooms in CF1 are likely due to poor preservation and a hiatus marked by an erosion surface just below the KTB indicating that the upper part of zone CF1 is missing. Globotruncanids are rare from the upper CF3 to the KTB, which most likely reflects the prevailing shallow environment. *Heterohelix* species inversely correlate with *Guembelitria* blooms, though *H. planata* is absent from CF2.

These faunal data indicate high-stress in a shallow water environment that excludes all deeper dwelling specialized taxa (globotruncanids) and in CF2 reduces low oxygen tolerant biserial species. Most unusual are the *Guembelitria* blooms in zone CF3, which are

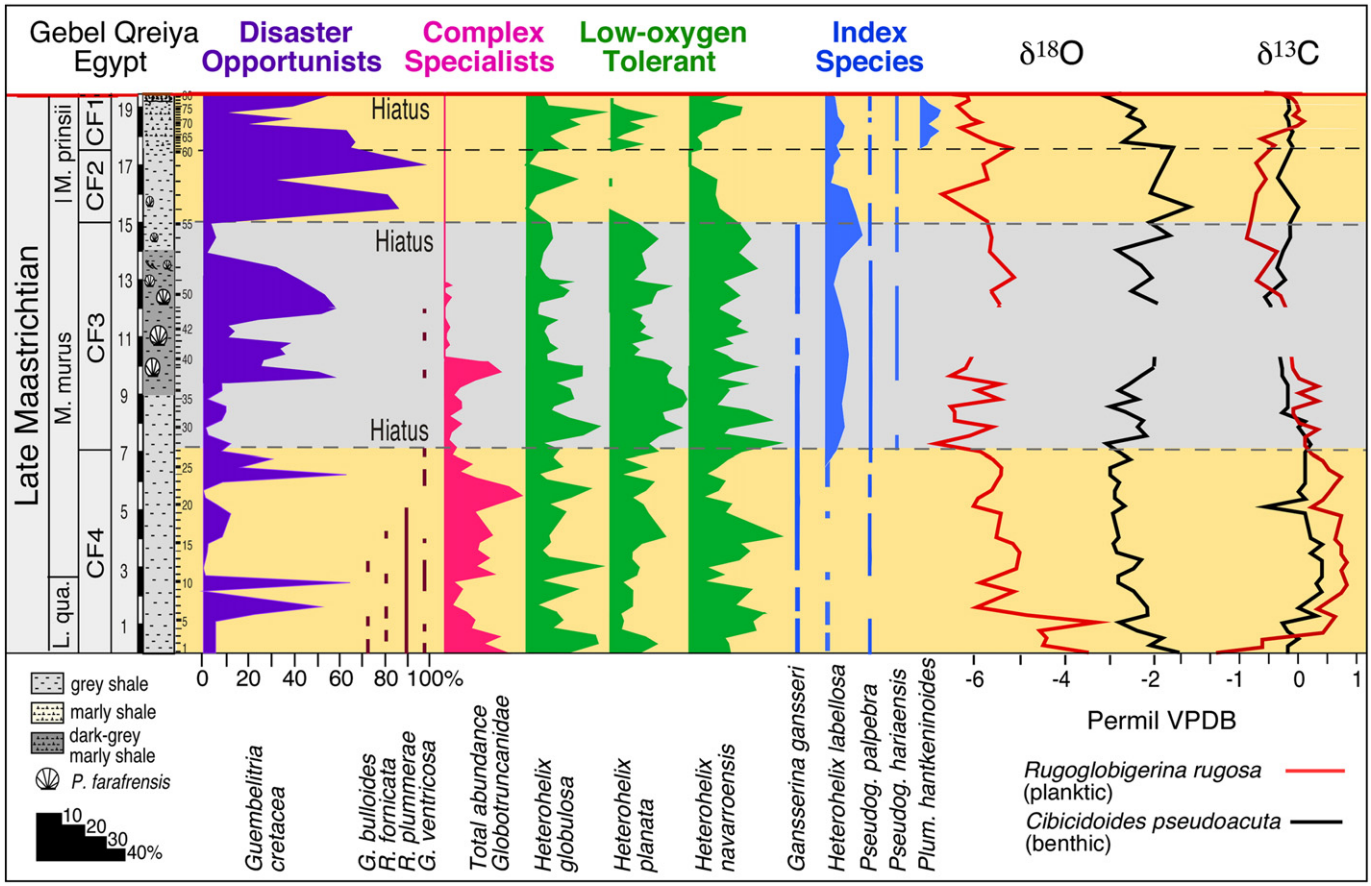

Fig. 9. Late Maastrichtian stable isotope and planktic foraminiferal stratigraphy of dominant species at Gebel Qreiya, Western Desert, Egypt (data from Keller (2002); Keller et al. (2002); Punekar et al. (2014b)). For explanation of species grouping see Fig. 6 caption. Dominant species are the same as in Israel and Madagascar though with some important differences: species abundances systematically vary inversely with *Guembelitria cretacea*. *Heterohelix (Spiroplecta) navarroensis* is abundant at Qreiya, though nearly absent in other sites, and Globotruncanidae species disappear by the middle of zone CF3. These faunal differences mainly reflect a shallowing sea and restricted influx of oceanic water in central Egypt. Stable isotope values are also variable, but climate and productivity trends are present. See text for interpretation.

not observed in Madagascar or Israel and suggest local high-stress conditions. Although CF3 *Guembelitria* blooms are present in the volcanic sediments of Site 216, their absence in CF3 elsewhere suggests that the blooms in Egypt are not related to this volcanic event. Keller (2002); Keller et al. (2002) suggested that CF3 high-stress conditions are likely related to the location of Qreiya on the southern margin of the sea subject to restricted seawater influx during the sea level low of CF3. This could lead to mesotrophic conditions due to nutrient build up from terrestrial influx (e.g., organic-rich dark shales in CF3) and create increasingly high-stress environments for marine plankton, excluding most species leading to *Guembelitria* blooms. Further clues to the nature of this environment can be obtained from the stable isotope record.

The $\delta^{13}C$ record shows most positive values in CF4 and decreasing in CF3 to CF1. Near the top of CF3, planktic values reverse the $\delta^{13}C$ gradient to more negative planktic than benthic values. This reversal can be explained by the relatively constant terrestrial ^{12}C influx and greater recrystallization of planktic tests due to their thinner and more porous wall structure (Keller et al., 2002; Stüben et al., 2003; Punekar et al., 2014b). The intervals of low $\delta^{13}C$ planktic values are correlative with major reduction in large specialized species (thermocline dwellers) and blooms (75–90%) of the disaster opportunist *Guembelitria* or low oxygen tolerant *Heterohelix* species. Keller et al. (2002) attributed these changes to the late Maastrichtian cooling and sea-level fall across the CF3–CF2 transition that resulted in restricted circulation in central and southern Egypt. Alternatively, Punekar et al. (2014b) suggested the low $\delta^{13}C$ values of Dissolved Inorganic Carbon (DIC) could reflect increased terrestrial weathering and detrital influx.

4. Discussion

4.1. Late Maastrichtian climate extremes

The generally cool Maastrichtian climate was interrupted by two rapid warm events at ~68–69.5 Ma (upper C31R to base C30n) and 66.25–66.00 Ma (C29r below KTB) and extreme faunal turnovers ending in the KTB mass extinction (Fig. 1) (e.g., Li and Keller, 1998a,b, 1999; Stüben et al., 2003; Isaza-Londoño et al., 2006). High atmospheric CO_2 prevailed with mean annual temperatures in west Texas up to 21–23 °C (at 35°N paleolatitude, Nordt et al., 2003).

Based on temperature calculations from marine and terrestrial environments (carbon and oxygen isotopes of foraminifera, pedogenic carbonate nodules, and plants) the latest Maastrichtian (CF2–CF1) greenhouse warming was attributed to Deccan volcanic degassing (Li and Keller, 1998b; Keller, 2001, 2005, 2014; Olsson et al., 2001; Nordt et al., 2003; Stüben et al., 2003; Isaza-Londoño et al., 2006; Robinson et al., 2009; Punekar et al., 2014a). The early late Maastrichtian warming was attributed to an abrupt reorganization of intermediate oceanic circulation (Abramovich et al., 1998, 2010; Frank and Arthur, 1999; Li and Keller, 1999; Keller, 2001), though this study suggests new likely causes for this climatic event (see Section 4.3).

4.2. Late Maastrichtian faunal upheavals

Extraordinary faunal upheavals in planktic foraminifera accompanied the late Maastrichtian climate extremes marking both the Cretaceous diversity maximum and the KTB mass extinction.

4.2.1. Diversity maximum — CF4

Anomalous during the early late Maastrichtian upheaval (~68–69.5 Ma) is the unprecedented rapid evolutionary diversification averaging 10 species per 500 ky compared with 2 species per 500 ky during the preceding cool interval. Planktic foraminifera reached maximum diversity in their history in the lower part of zone CF4 near the top of C31n (Li and Keller, 1998a; Keller, 2001) (Fig. 1). Total diversity at Site 525A increased by 43%, primarily in large complex morphologies. Globotruncanids (intermediate or thermocline dwellers) increased from 16 to 26 species and surface dwellers parallel this trend increasing from 12 to 21 species (Li and Keller, 1998a,c, 1999; Keller, 2001) (Fig. 1). This diversity extreme is also observed in Sites 21 and 463, Tunisia, Madagascar, Israel, and in deep wells from the Cauvery Basin, India, and is generally recorded in Maastrichtian assemblages of low and middle latitudes (Abramovich et al., 1998, 2002, 2010; Li and Keller, 1998a,c).

Several factors explain the diversity maximum, including diversity depletion after the Campanian to Maastrichtian cooling that reduced competition, and well-stratified warm oceans with expanded intermediate and surface mixed layers ideal for evolutionary diversification, particularly in the absence of competition. However, such rapid diversity increase over a short warm interval is unusual, thereby indicating other factors such as increased humidity and runoff of nutrients into the oceans and/or nutrient input from volcanic sources (e.g., Deccan Traps, Ninetyeast Ridge).

4.2.2. Diversity decline

The diversity decline began at the top of C31n near the end of the early late Maastrichtian warming (Fig. 1) with selective extinctions of large complex holdover survivors from the warmer Campanian, especially *G. bulloides*, *C. fornicata* and *C. plummerae* (Fig. 5), and possibly also *G. wiedenmayeri*, *A. cretacea* and *Contusotruncana plicata*. However, the total abundance of globotruncanids suffered sharp drops from typical 30–40% pre-warming to ~20% during the CF4 warm event and diversity varied significantly (Fig. 10). Decreased diversity and abundance of large complex species can be attributed to decreased water mass stratification associated with the onset of cooling. Calcareous nannofossil assemblages record no obvious change in species richness for the CF4 warm event (Thibault and Gardin, 2006; Sheldon et al., 2010; Thibault et al., 2015b) although a significant decline begins within UC20b near the CF4–CF3 transition in the tropical Pacific and South Atlantic (Thibault and Gardin, 2010).

4.2.3. Guembelitria blooms and volcanism

From India to Ninetyeast Ridge, Madagascar, Israel and Texas, *Guembelitria* blooms are at a maximum in the Indian Ocean and decrease westward. Their abundance peaks are correlative with rapid greenhouse warming during Deccan eruptions phase-2 and phase-3 (Fig. 11) (review in Punekar et al. (2014a)). The CF4 rapid warming and faunal upheaval is also dominated by *Guembelitria* blooms with maximum abundance (80–90%) in the volcanic sediments of Site 216 on Ninetyeast Ridge and decreasing westward (Fig. 11). During this time both Ninetyeast Ridge volcanism and Deccan Traps phase-1 were active. Similar trends are observed for Deccan phase-2 (C29r, CF2–CF1) where blooms in India dominate (>90%) but the westward decrease is much less (50–60%) in Israel and Texas (note the low abundance in CF2–CF1 in Madagascar due to an incomplete record). *Guembelitria* blooms are also correlative with Deccan phase-3 and the early Danian DanC2 warm event (zone P1b, C29n) as recorded from India to the eastern Tethys to Texas. However in Texas, *Guembelitria's* evolutionary descendant, *Globoconusa daubjergensis* dominates assemblages though indicating similar high-stress conditions (review in Punekar et al. (2014a)).

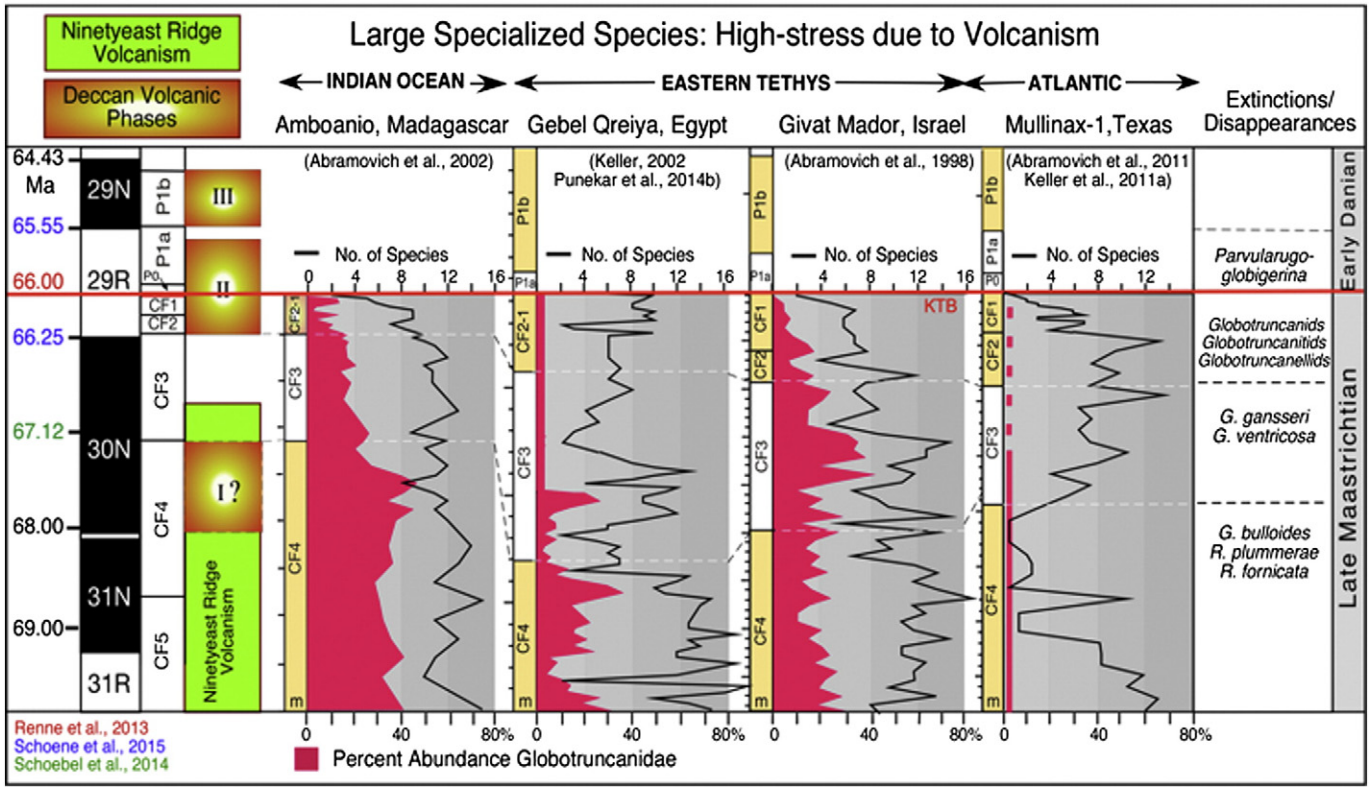

Fig. 10. Abundance and diversity of large specialized species, predominantly Globotruncanidae, during the late Maastrichtian from the Indian Ocean to the eastern Tethys and Texas correlative with Deccan phase-1 (CF4), phase-2 (CF2–CF1) and Ninetyeast Ridge (Kerguelen hotspot) volcanism. Decreased abundance in the upper zone CF4 leading to the mass extinction reflects high-stress conditions; a temporary increase in the upper CF4 at Givat Mador is likely due to local conditions; the near absence of Globotruncanidae in Texas reflects a shallow sea. Fluctuating species diversity reflects stress conditions at each locality.

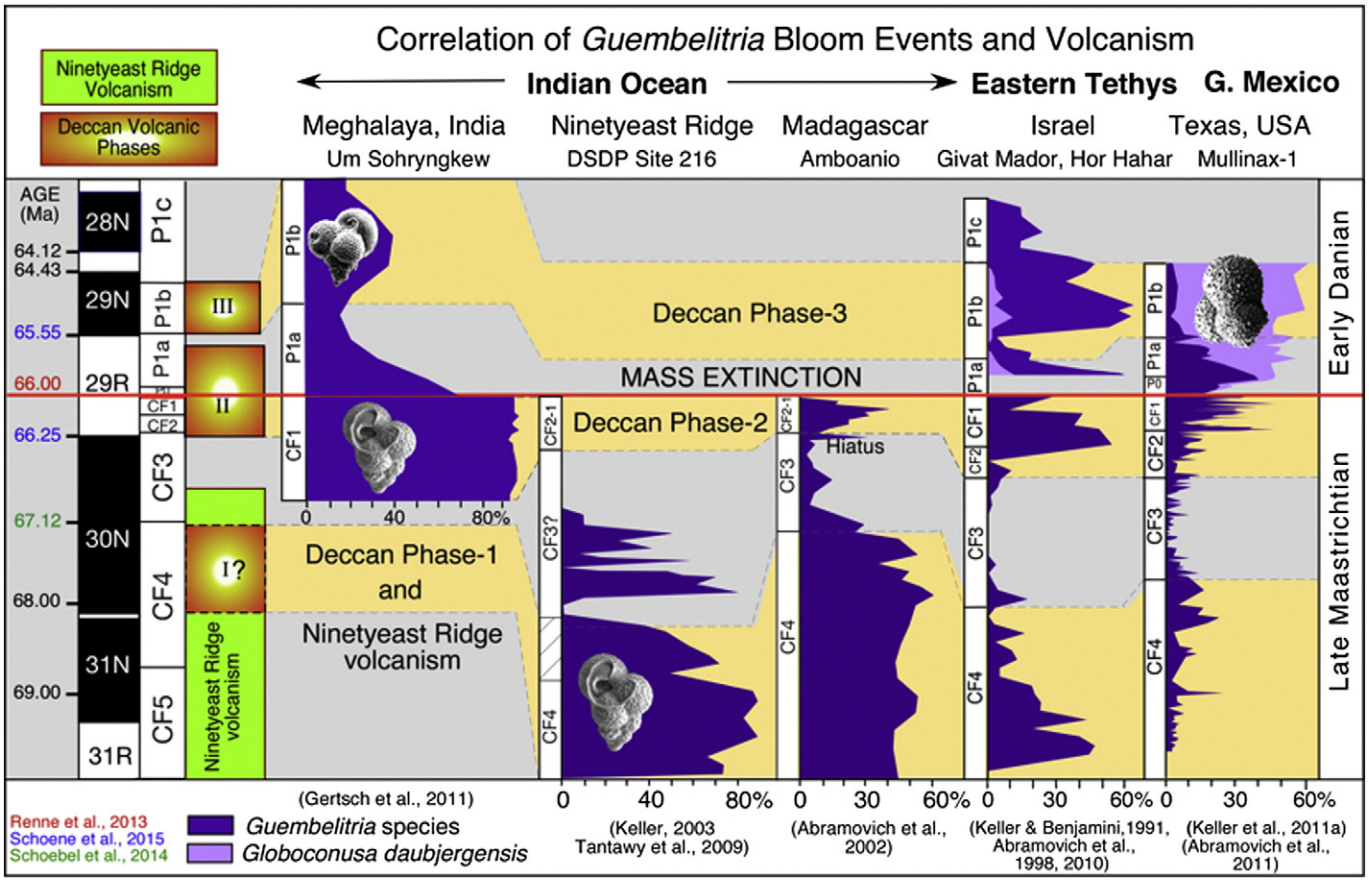

Fig. 11. *Guembelitria* bloom events from Madagascar to Texas correlative with Deccan phase-1 (CF4, C30n), phase-2 (CF2-CF1, C29r), phase-3 (P1b, C29n) and Ninetyeast Ridge (Kerguelen hotspot) volcanism. The largest blooms are in the latest Maastrichtian zones CF2–CF1, correlative with C29r and Deccan phase-2 below the mass extinction. In Madagascar the CF2–CF1 blooms are relatively small because most of this interval is missing and preservation is poor (Abramovich et al., 2002). The highest CF2–CF1 blooms are observed in Meghalaya, India and the eastern Tethys (Abramovich et al., 1998; Keller, 2002; Punekar et al., 2014b). CF4 blooms are most dominant (80–90%) on Ninetyeast Ridge Site 216 under the influence of Kerguelen hotspot volcanism, but significantly smaller and decreasing westwards (Texas) suggesting lower environmental stress conditions compared with phase-2.

Guembelitria species are known as ecological disaster opportunists able to thrive in high-stress environments that led to the exclusion of other species. They are small surface dwellers with simple morphology and thin-walled globular chambers arranged in triserial form. Their opportunistic R-selected life strategy of rapid reproduction, large numbers of offspring, and wide range of tolerance to unstable environments optimizes chances of survival. *Guembelitria* blooms were first recorded in early Danian zones P0–P1a in the aftermath of the KTB mass extinction (Luciani, 2002; Keller and Pardo, 2004; Coccioni and Luciani, 2006). Even larger blooms were discovered in association with the latest Maastrichtian C29r, zones CF2–CF1 rapid greenhouse warming linked to Deccan volcanism phase-2 leading up to the mass extinction (review in Pardo and Keller (2008)). More recently, *Guembelitria* blooms were documented from the early Danian zone P1b (C29n) associated with the Dan-C2 rapid warming, which is correlative with Deccan volcanism phase-3 (Quillévéré et al., 2008). The full recovery of planktic foraminifera begins only after this climate warming nearly 1 my after the mass extinction (Punekar et al., 2014a). *Guembelitria* blooms have also been documented in zone CF4 (middle C31n to lower C30n) also associated with rapid greenhouse warming possibly related to volcanic outgassing (phase-1).

4.3. Correlation with Deccan phase-1 and Ninetyeast Ridge volcanism

All three *Guembelitria* bloom events are associated with rapid climate warming, and two of these are already demonstrated to coincide with Deccan volcanism phase-2 and phase-3, which suggests that phase-1 may be the cause for the extreme faunal upheaval in zone CF4 (Fig. 11). The age and duration of phase-1 are still uncertain. $^{40}Ar/^{39}Ar$ ages of 67.5 ± 0.6 Ma (Chenet et al., 2007) and 67.12 ± 0.44 Ma (Schöbel et al., 2014) have been proposed for the oldest Deccan eruptions, which are considered the smallest of the three Deccan phases accounting for just 6% of the total eruptions by volume (Chenet et al., 2007, 2008). If this estimate is correct, it is doubtful that the observed warming or faunal upheaval could have been caused by the onset of Deccan phase-1. However, Deccan phase-1 eruptions are least known and high-precision dating (U–Pb) still remains to be done to evaluate the volume, rate and tempo of eruptions. We can infer the potential duration of Deccan phase-1 as at least 0.5–1.0 my based on *Guembelitria* blooms in CF4, and the onset of climate warming as early as ~69.5 Ma and lasting 1.5 million years.

Alternatively, Ninetyeast Ridge volcanism may have preceded and/or overlapped Deccan phase-1 (Figs. 7, 11). There is support for Ninetyeast Ridge volcanism preceding or cotemporaneous with Deccan phase-1 based on biostratigraphy and high-stress assemblages at Site 216 (Fig. 7) (Keller, 2003). The Kerguelen hotspot that formed Ninetyeast Ridge erupted at DSDP Site 216 (Fig. 2) sometime during the Maastrichtian and deposited amygdalar and vesicular basalt above the basement basalt. Calcareous nannofossils in the basal part of these volcanic sediments indicate a late Maastrichtian (zone UC20a) age, equivalent to planktic foraminiferal zones CF5–CF4 or about 69.5 Ma (Fig. 4) (Keller, 2003; Tantawy et al., 2009). This is a very close match with the onset of climate warming near the base of CF5 estimated at ~69.5 Ma at Site 525A (Fig. 1).

The extreme high-stress conditions at Site 216 with *Guembelitria* blooms dominating (80–90%) and alternating with low oxygen tolerant

Heterohelix species and few other survivors mark Ninetyeast Ridge volcanic eruptions for at least 2 million years. During this time, marine stress conditions were vastly more intense than at other localities, including India (Cauvery Basin) and Madagascar (Fig. 11). These data suggest that Ninetyeast Ridge volcanism during the late Maastrichtian was a significant contributor to global environmental stress and appears to have both preceded and overlapped Deccan volcanism phase-1. High precision age dating is needed for both Ninetyeast Ridge and Deccan phase-1 volcanism to determine the precise age, tempo and duration of eruptions in order to evaluate their respective contributions to the late Maastrichtian faunal upheavals.

4.4. Implications for the Chicxulub impact

The Chicxulub impact is a single instantaneous event that cannot account for the observed long-term environmental changes. Was Chicxulub the sole cause for the mass extinction as has been claimed for the past 35 years? The answer is unequivocally NO. Deccan phase-2 eruptions beginning at 66.250 Ma (base C29r, Schoene et al., 2015) directly led to the KTB mass extinction as documented from intertrappean sediments in deep wells from the Krishna-Godavari Basin (Keller et al., 2011b, 2012; Keller, 2014). Could the Chicxulub impact have contributed to this mass extinction? Yes, of course. It could have exacerbated the already catastrophic conditions due to Deccan eruptions – if the impact predates the mass extinction. There is strong, even overwhelming evidence from impact glass spherules in NE Mexico and Texas that the Chicxulub impact predates the mass extinction by possibly as much as 80–100 ky based on current dating (Keller et al., 2009a, 2011a, 2013).

4.4.1. Chicxulub as trigger for Deccan killer eruptions?

Richards et al. (2015) suggest that the coincident of "a sudden outburst of Deccan eruptions occurring within ~100,000 yr or less of the Cretaceous–Paleogene time and accounting for >70% of the Deccan main phase eruptions would seem to have a miniscule chance of occurring at random." They propose that the Chicxulub impact triggered this massive pulse of eruptions and may have caused volcanic eruptions worldwide, though they admit that no data exists to support this idea at this time. It is interesting that in this scenario the Chicxulub impact is presumed to predate the mass extinction by up to 100,000 years – which has been suggested by Keller et al. (2002, 2004, 2009 and references therein) based on biostratigraphy, magnetostratigraphy, sedimentology and geochemistry of numerous sequences in NE Mexico and Texas.

Meschede et al. (2011) investigated the global seismic effects of the Chicxulub impact and found that the shock waves would have to be bundled to their greatest effect at the precise opposite side of the planet, the antipode. The antipode of Yucatan 66 million years ago was Indonesia–India was as much as 6000 km away. This means that the impact was not likely to have had a significant effect on Deccan volcanism.

Ultimately, high precision U–Pb dating of the massive Deccan lava flows is necessary to develop the chronology of the Deccan eruptions during the last 250 ky of the Cretaceous and particularly to date the four longest lava flows that record the mass extinction in the intertrappean sediments (Keller et al., 2011b, 2012). However, even this high precision dating can provide no evidence that the Chicxulub impact triggered the lava flows that caused the mass extinction. Moreover, we cannot assume that the world's longest lava flows just prior to the mass extinction were triggered or amplified by the Chicxulub impact because similar massive volcanic eruptions resulting in another 3–4 equally long lava flows occurred in the early Danian (base C29n) Deccan phase-3 about 500 ky after the mass extinction (review in Punekar et al. (2014a)).

5. Conclusions

Evaluation of high-stress planktic foraminiferal assemblages from the Indian Ocean to the Eastern Tethys and Gulf of Mexico (Texas) during the late Maastrichtian reveals two faunal upheavals during rapid climate warming, each associated with major volcanism.

The early late Maastrichtian warming of 2–3 °C in intermediate waters spans from ~69.5 to 68 Ma (upper C31r to base C30n, zones CF5–CF4) and resulted in rapid evolutionary diversification in intermediate and surface waters increasing species assemblages by 43% marking the highest planktic foraminifer diversity in their history. At the same time high-stress conditions prevailed in surface and subsurface waters as marked by blooms of the disaster opportunist *Guembelitria* blooms and low oxygen tolerant small *Heterohelix* species.

This evolution streak ends abruptly near the end of the warm event (top C31n) with a cluster of extinctions marking the onset of the terminal diversity decline that ends at the KTB mass extinction.

The early late Maastrichtian climate warming and faunal upheaval correlate with major volcanic activity at DSDP Site 216 on Ninetyeast Ridge (Kerguelen hotspot) where volcanic sediments above basement basalt are dated ~69.5 Ma (nannofossil zone UC20a, planktic foraminiferal zones CF5–CF4) and continued for about 2 million years. Deccan volcanism (phase-1) also began during this time interval although we are still uncertain about their age and duration.

The latest Maastrichtian warm event in C29r (zones CF2–CF1, UC20d) increased intermediate water temperatures by 3–4 °C and resulted in extreme stress conditions marked by *Guembelitria* blooms, species dwarfing, reduced diversity and abundances of specialized species that ended with rapid mass extinction of nearly all species. Documentation of the mass extinction in intertrappean sediments between massive Deccan lava flows reveals Deccan volcanism phase-2 as the cause for the rapid warming and mass extinction.

Global warming and high-stress conditions associated with early late and latest Maastrichtian volcanic events, are marked by *Guembelitria* blooms and reduced diversity and abundance of large specialized species particularly Globotruncanidae, with stress conditions at a maximum near volcanic centers and diminishing with distance. The highest stress condition (maximum *Guembelitria* blooms) mark maximum warming in C29r prior to the rapid mass extinction.

Massive Deccan outgassing, climate warming and ocean acidification at the end of the Maastrichtian appear to be the direct causes for the mass extinction. The Chicxulub impact, now considered to predate the mass extinction by ~100 ky may have contributed to this catastrophe but was not likely the cause.

Acknowledgments

We are grateful to the anonymous reviewers for their very helpful comments and critiques. This study is based upon work originally supported by the US National Science Foundation through the Continental Dynamics Program, Sedimentary Geology and Paleobiology Program and Office of International Science & Engineering's India Program under NSF grants EAR-0207407, EAR-0447171, and EAR-1026271.

References

Abramovich, S., Keller, G., 2002. High stress late Maastrichtian paleoenvironment: inference from planktonic foraminifera in Tunisia. Palaeogeogr. Palaeoclimatol. Palaeoecol. 178, 145–164. http://dx.doi.org/10.1016/S0031-0182(01)00394-7.

Abramovich, S., Keller, G., 2003. Planktonic foraminiferal response to the latest Maastrichtian abrupt warm event: a case study from South Atlantic DSDP Site 525A. Mar. Micropaleontol. 48, 225–249. http://dx.doi.org/10.1016/S0377-8398(03)00021-5.

Abramovich, S., Almongi-Labin, A., Benjamini, C., 1998. Decline of the Maastrichtian pelagic ecosystem based on planktic foraminifera assemblage changes: implication for the terminal Cretaceous faunal crisis. Geology 26, 63–66. http://dx.doi.org/10.1130/0091-7613(1998)026<0063:DOTMPE>2.3.CO;2.

Abramovich, S., Keller, G., Adatte, T., Stinnesbeck, W., Hottinger, L., Stüben, D., Berner, Z., Ramanivosoa, B., Randriamanantenasoa, A., 2002. Age and paleoenvironment of the Maastrichtian–Paleocene of the Mahajanga Basin, Madagascar: a multidisciplinary approach. Mar. Micropaleontol. 47, 17–70. http://dx.doi.org/10.1016/S0377-8398(02)00094-4.

Abramovich, S., Keller, G., Stüben, D., Berner, Z., 2003. Characterization of late Campanian and Maastrichtian planktonic foraminiferal depth habitats and vital activities based

on stable isotopes. Palaeogeogr. Palaeoclimatol. Palaeoecol. 202, 1–29. http://dx.doi.org/10.1016/S0031-0182(03)00572-8.
Abramovich, S., Yovel-Corem, S., Almogi-Labin, A., Benjamini, C., 2010. Global climate change and planktic foraminiferal response in the Maastrichtian. Paleoceanography 25, PA2201. http://dx.doi.org/10.1029/2009PA001843.
Abramovich, S., Keller, G., Berner, Z., Cymbalista, M., Rak, C., 2011. Maastrichtian planktic foraminiferal biostratigraphy and paleoenvironment of Brazos River, Falls County, Texas. In: Keller, G., Adatte, T. (Eds.), The End-Cretaceous Mass Extinction and the Chicxulub Impact in Texas. Society for Sedimentary Geology Special Publication 100. ISBN: 978-1-56576-308-1, pp. 123–156.
Adatte, T., Keller, G., Burns, S., Stoykova, K.H., Ivanov, M.I., Vangelov, D., Kramar, U., Stüben, D., 2002. Paleoenvironment across the Cretaceous–Tertiary transition in eastern Bulgaria. Geol. Soc. Am. Spec. Pap. 356, 231–251. http://dx.doi.org/10.1130/0-8137-2356-6.231.
Almogi-Labin, A., Flexer, A., Honigstein, A., Rosenfeld, A., Rosenthal, E., 1990. Biostratigraphy and tectonically controlled sedimentation of the Maastrichtian in Israel and adjacent countries. Rev. Esp. Paleontol. 5, 41–52.
Barrera, E., 1994. Global environmental changes preceding the Cretaceous–Tertiary boundary: Early late Maastrichtian transition. Geology 22, 877–880. http://dx.doi.org/10.1130/0091-7613(1994)022<0877:GECPTC>2.3.CO;2.
Barrera, E., Savin, S.M., Thomas, E., Jones, C.E., 1997. Evidence for thermohaline-circulation reversals controlled by sea-level change in the latest Cretaceous. Geology 25, 715–718. http://dx.doi.org/10.1130/0091-7613(1997)025<0715:EFTCRC>2.3.CO;2.
Burnett, J., 1998. Upper Cretaceous. In: Bown, P.R. (Ed.), Calcareous Nannofossil Biostratigraphy. Chapman & Hall, Cambridge, pp. 132–199.
Camoin, G., Bellion, Y., Benkhelil, J., Cornée, J.-J., Dercourt, J., Guiraud, R., Poisson, A., Vrielynck, B., 1993. Late Maastrichtian palaeoenvironments (69.5 to 65 Ma). In: Dercourt, J., Ricou, L.E., Vrielynck, B. (Eds.), Atlas Tethys Paleoenvironmental Maps. Beicip-Franlab, Rueil-Malmaison, France, pp. 179–196.
Chenet, A.-L., Quidelleur, X., Fluteau, F., Courtillot, V., Bajpai, S., 2007. $^{40}K/^{40}Ar$ dating of the main Deccan large igneous province: further evidence of Cretaceous–Tertiary boundary age and short duration. Earth Planet. Sci. Lett. 263, 1–15. http://dx.doi.org/10.1016/j.epsl.2007.07.011.
Chenet, A.-L., Fluteau, F., Courtillot, V., Gerard, M., Subbarao, K.V., 2008. Determination of rapid Deccan eruptions across the Cretaceous–Tertiary boundary using paleomagnetic secular variation: results from a 1200-m-thick section in the Mahabaleshwar. J. Geophys. Res. 113, B04101. http://dx.doi.org/10.1029/2006JB004635.
Chenet, A.-L., Courtillot, V., Fluteau, F., Gerard, M., Quidelleur, X., Khadri, S.F.R., Subbarao, K.V., Thordarson, T., 2009. Determination of rapid Deccan eruptions across the Cretaceous–Tertiary boundary using paleomagnetic secular variation: 2. Constraints from analysis of eight new sections and synthesis for a 3500-m-thick composite section. J. Geophys. Res. 114, B06103. http://dx.doi.org/10.1029/2008JB005644.
Coccioni, R., Luciani, R., 2006. *Guembelitria irregularis* bloom at the K-T boundary: morphological abnormalities induced by impact-related extreme environmental stress? In: Cockell, C., Koeberl, C., Gilmour, I. (Eds.), Biological Processes Associated with Impact Events. Springer, Berlin, Heidelberg, pp. 179–196 http://dx.doi.org/10.1007/3-540-25736-5_8
Coccioni, R., Premoli Silva, I., 2015. Revised Upper Albian–Maastrichtian planktonic foraminiferal biostratigraphy and magnetostratigraphy of the classical Tethyan Gubbio section (Italy). Newsl. Stratigr. 48, 47–90.
Courtillot, V., Fluteau, F., 2014. A review of the embedded time scales of flood basalt volcanism with special emphasis on dramatically short magmatic pulses. In: Keller, G., Kerr, A.C. (Eds.), Volcanism, Impacts, and Mass Extinctions: Causes and Effects. Geological Society of America Special Paper 505, pp. SPE505–SPE515. http://dx.doi.org/10.1130/2014.2505(15).
Duncan, R.A., 1978. Geochronology of basalts from the Ninetyeast Ridge and continental dispersion in the eastern Indian Ocean. J. Volcanol. Geotherm. Res. 4, 283–305.
Duncan, R.A., 1991. Age distribution of volcanism along aseismic ridges in the eastern Indian Ocean. Proc. Ocean Drill. Program 121, 507–517. http://dx.doi.org/10.2973/odp.proc.sr.121.162.1991.
Font, E., Nedelec, A., Ellwood, B.B., Mirao, J., Silva, P.F., 2011. A new sedimentary benchmark for the Deccan Traps volcanism? Geophys. Res. Lett. 38, L24309. http://dx.doi.org/10.1029/2011GL049824.
Font, E., Fabre, S., Nédélec, A., Adatte, T., Keller, G., Veiga-Pires, C., Ponte, J., Mirão, J., Khozyem, H., Spangenberg, J., 2014. Atmospheric halogen and acid rains during the main phase of Deccan eruptions: magnetic and mineral evidence. In: Keller, G., Kerr, A.C. (Eds.), Volcanism, Impacts and Mass Extinctions: Causes and Effects. Geological Society of America Special Paper 505, pp. SPE505–SPE518. http://dx.doi.org/10.1130/2014.2505(18).
Frank, D.T., Arthur, M.A., 1999. Tectonic forcings of Maastrichtian ocean-climate evolution. Paleoceanography 14, 103–117.
Frey, F.A., Pringle, M., Meleney, P., Huang, S., Piotrowski, A., 2011. Diverse mantle sources for Ninetyeast Ridge magmatism: geochemical constraints from basaltic glasses. Earth Planet. Sci. Lett. 303, 215–224. http://dx.doi.org/10.1016/j.epsl.2010.12.051.
Friedrich, O., Herrle, J.O., Wilson, P.A., Cooper, M.J., Erbacher, J., Hemleben, C., 2009. Early Maastrichtian carbon cycle perturbation and cooling event: implications from the South Atlantic Ocean. Paleoceanography 24, PA2211. http://dx.doi.org/10.1029/2008PA001654.
Gardin, S., Galbrun, B., Thibault, N., Coccioni, R., Premoli Silva, I., 2012. Biomagnetochronology for the upper Campanian–Maastrichtian from the Gubbio area, Italy: new results from the Contessa Highway and Bottaccione sections. Newsl. Stratigr. 45, 75–100. http://dx.doi.org/10.1127/0078-0421/2012/0014.
Gertsch, B., Keller, G., Adatte, T., Garg, R., Prasad, V., Fleitmann, D., Berner, Z., 2011. Environmental effects of Deccan volcanism across the Cretaceous–Tertiary transition in Meghalaya, India. Earth Planet. Sci. Lett. 310, 272–285. http://dx.doi.org/10.1016/j.epsl.2011.08.015.
Haq, B.U., 2014. Cretaceous eustasy revisited. Glob. Planet. Chang. 113, 44–58. http://dx.doi.org/10.1016/j.gloplacha.2013.12.007.
Hendriks, F., Luger, P., Biwitz, J., Kallenbach, H., 1987. Evolution of the depositional environments of SE Egypt during the Cretaceous and lower Tertiary. Berl. Geowiss. Abh. A75, 49–82.
Husson, D., Galbrun, B., Laskar, J., Hinnov, L.A., Thibault, N., Gardin, S., Locklair, R.E., 2011. Astronomical calibration of the Maastrichtian (late Cretaceous). Earth Planet. Sci. Lett. 305, 328–340. http://dx.doi.org/10.1016/j.epsl.2011.03.008.
Isaza-Londoño, C., MacLeod, K.G., Huber, B.T., 2006. Maastrichtian North Atlantic warming, increasing stratification, and foraminiferal paleobiology at three timescales. Paleoceanography 21, PA1012. http://dx.doi.org/10.1029/2004PA001130.
Keller, G., 1993. The Cretaceous–Tertiary boundary transition in the Antarctic Ocean and its global implications. Mar. Micropaleontol. 21, 1–45. http://dx.doi.org/10.1016/0377-8398(93)90010-U.
Keller, G., 2001. The end-Cretaceous mass extinction in the marine realm: year 2000 assessment. Planet. Space Sci. 49, 817–830. http://dx.doi.org/10.1016/S0032-0633(01)00032-0.
Keller, G., 2002. *Guembelitria*-dominated late Maastrichtian planktic foraminiferal assemblages mimic early Danian in central Egypt. Mar. Micropaleontol. 47, 71–99. http://dx.doi.org/10.1016/S0377-8398(02)00116-0.
Keller, G., 2003. Biotic effects of impacts and volcanism. Earth Planet. Sci. Lett. 215, 249–264. http://dx.doi.org/10.1016/S0012-821X(03)00390-X.
Keller, G., 2004. Paleoecology of Late Maastrichtian–early Danian planktic foraminifera in the eastern Tethys. J. Foraminifer. Res. 34, 49–73.
Keller, G., 2005. Biotic effects of late Maastrichtian mantle plume volcanism: implications for impacts and mass extinctions. Lithos 79, 317–341. http://dx.doi.org/10.1016/j.lithos.2004.09.005.
Keller, G., 2011. The KT Mass Extinction: Theories and Controversies. In: Keller, G., Adatte, T. (Eds.), The End-Cretaceous Mass Extinction and the Chicxulub Impact in Texas. Society for Sedimentary Geology Special Publication 100, pp. 7–22.
Keller, G., 2014. Deccan volcanism, the Chicxulub impact and the end-Cretaceous mass extinction: coincidence? Cause and effect? In: Keller, G., Kerr, A.C. (Eds.), Volcanism, Impacts, and Mass Extinctions: Causes and Effects. Geological Society of America Special Paper 505, pp. 57–89. http://dx.doi.org/10.1130/2014.2505(03)
Keller, G., Abramovich, S., 2009. Lilliput effect in late Maastrichtian planktic foraminifera: response to environmental stress. Palaeogeogr. Palaeoclimatol. Palaeoecol. 284, 47–62. http://dx.doi.org/10.1016/j.palaeo.2009.08.029.
Keller, G., Benjamini, C., 1991. Paleoenvironment of the eastern Tethys in the early Danian. Palaios 6, 439–464. http://dx.doi.org/10.2307/3514984.
Keller, G., Pardo, A., 2004. Disaster opportunists Guembelitrinidae — index for environmental catastrophes. Mar. Micropaleontol. 53, 83–116. http://dx.doi.org/10.1016/j.marmicro.2004.04.012.
Keller, G., Benjamini, C., Magaritz, M., Moshkovitz, S., 1991. Faunal, erosional and $CaCO_3$ events in the Early Tertiary Eastern Tethys. In: Sharpton, V.L., Ward, P.D. (Eds.), Global Catastrophes in Earth History. Geological Society of America Special Paper 247, pp. 471–480.
Keller, G., Adatte, T., Burns, S.J., Tantawy, A., 2002. High stress paleoenvironment during the late Maastrichtian to early Paleocene in Central Egypt. Palaeogeogr. Palaeoclimatol. Palaeoecol. 187, 35–60. http://dx.doi.org/10.1016/S0031-0182(02)00504-7.
Keller, G., Adatte, T., Stinnesbeck, W., Rebolledo-Vieyra, M., Urrutia Fucugauchi, J., Kramar, U., Stüben, D., 2004. Chicxulub impact predates K-T boundary mass extinction. Proc. Natl. Acad. Sci. U. S. A. 101, 3753–3758. http://dx.doi.org/10.1073/pnas.0400396101.
Keller, G., Adatte, T., Tantawy, A.A., Berner, Z., Stüben, D., 2007. High stress late Cretaceous to early Danian paleoenvironment in the Neuquen Basin, Argentina. Cretac. Res. 28, 939–960. http://dx.doi.org/10.1016/j.cretres.2007.01.006.
Keller, G., Adatte, T., Gardin, S., Bartolini, A., Bajpai, S., 2008. Main Deccan volcanism phase ends near the K-T boundary: evidence from the Krishna-Godavari Basin, SE India. Earth Planet. Sci. Lett. 268, 293–311. http://dx.doi.org/10.1016/j.epsl.2008.01.015.
Keller, G., Adatte, T., Berner, Z., Pardo, A., Lopez-Oliva, J.G., 2009a. New evidence concerning the age and biotic effects of the Chicxulub impact in NE Mexico. J. Geol. Soc. 166, 393–411. http://dx.doi.org/10.1144/0016-76492008-116.
Keller, G., Khosla, S.C., Sharma, R., Khosla, A., Bajpai, S., Adatte, T., 2009b. Early Danian planktic foraminifera from Cretaceous–Tertiary intertrappean beds at Jhilmili, Chhindwara District, Madhya Pradesh, India. J. Foraminifer. Res. 39, 40–55. http://dx.doi.org/10.2113/gsjfr.39.1.40.
Keller, G., Abramovich, S., Adatte, T., Berner, Z., 2011a. Biostratigraphy, age of the Chicxulub impact, and depositional environment of the Brazos River KTB sequences. In: Keller, G., Adatte, T. (Eds.), The End-Cretaceous Mass Extinction and the Chicxulub Impact in Texas. Society for Sedimentary Geology Special Publication 100. ISBN: 978-1-56576-308-1, pp. 81–122.
Keller, G., Bhowmick, P.K., Upadhyay, H., Dave, A., Reddy, A.N., Jaiprakash, B.C., Adatte, T., 2011b. Deccan volcanism linked to the Cretaceous–Tertiary boundary mass extinction: new evidence from ONGC wells in the Krishna-Godavari Basin. J. Geol. Soc. India 78, 399–428. http://dx.doi.org/10.1007/s12594-011-0107-3.
Keller, G., Adatte, T., Bhowmick, P.K., Upadhyay, H., Dave, A., Reddy, A.N., Jaiprakash, B.C., 2012. Nature and timing of extinctions in Cretaceous–Tertiary planktic foraminifera preserved in Deccan intertrappean sediments of the Krishna-Godavari Basin, India. Earth Planet. Sci. Lett. 341–344, 211–221. http://dx.doi.org/10.1016/j.epsl.2012.06.021.
Keller, G., Khozyem, H., Adatte, T., Malarkodi, N., Spangenberg, J.E., Stinnesbeck, W., 2013. Chicxulub impact spherules in the North Atlantic and Caribbean: age constraints and Cretaceous–Tertiary boundary hiatus. Geol. Mag. 150, 885–907. http://dx.doi.org/10.1017/S0016756812001069.
Krishna, K.S., Abraham, H., Sager, W.W., Pringle, M.S., Frey, F., Gopala Rao, D., Levchenko, O.V., 2012. Tectonics of the Ninetyeast Ridge derived from spreading records in adjacent oceanic basins and age constraints of the ridge. J. Geophys. Res. 117, B04101. http://dx.doi.org/10.1029/2011JB008805.

Li, L., Keller, G., 1998b. Maastrichtian climate, productivity and faunal turnovers in planktic foraminifera in South Atlantic DSDP Sites 525A and 21. Mar. Micropaleontol. 33, 55–86. http://dx.doi.org/10.1016/S0377-8398(97)00027-3.
Li, L., Keller, G., 1998a. Abrupt deep-sea warming at the end of the Cretaceous. Geology 26, 995–998. http://dx.doi.org/10.1130/0091-7613(1998)026<0995:ADSWAT>2.3.CO;2.
Li, L., Keller, G., 1998c. Diversification and extinction in Campanian–Maastrichtian planktic foraminifera of northwestern Tunisia. Eclogae Geol. Helv. 91, 75–102.
Li, L., Keller, G., 1999. Variability in Late Cretaceous climate and deep waters: evidence from stable isotopes. Mar. Geol. 161, 171–190. http://dx.doi.org/10.1016/S0025-3227(99)00078-X.
Li, L., Keller, G., Stinnesbeck, W., 1999. The late Campanian and Maastrichtian in northwestern Tunisia: paleoenvironmental inferences from lithology, macrofauna and benthic foraminifera. Cretac. Res. 20, 231–252. http://dx.doi.org/10.1006/cres.1999.0148.
Li, L., Keller, G., Adatte, T., Stinnesbeck, W., 2000. Late Cretaceous sea-level changes in Tunisia: a multi-disciplinary approach. J. Geol. Soc. Lond. 157, 447–458.
Luciani, V., 2002. High-resolution planktonic foraminiferal analysis from the Cretaceous–Tertiary boundary at Ain Settara (Tunisia): evidence of an extended mass extinction. Palaeogeogr. Palaeoclimatol. Palaeoecol. 178, 299–319. http://dx.doi.org/10.1016/S0031-0182(01)00400-X.
MacLeod, N., Keller, G., 1991. Hiatus distributions and mass extinctions at the Cretaceous/Tertiary boundary. Geology 19, 497–501. http://dx.doi.org/10.1130/0091-7613(1991)019<0497:HDAMEA>2.3.CO;2.
MacLeod, K.G., Huber, B.T., Isaza-Londoño, C., 2005. North Atlantic warming during global cooling at the end of the Cretaceous. Geology 33, 437–440. http://dx.doi.org/10.1130/G21466.1.
Magaritz, M., Benjamini, C., Keller, G., Moshkovitz, S., 1992. Early diagenetic isotopic signal at the Cretaceous/Tertiary boundary, Israel. Palaeogeogr. Palaeoclimatol. Palaeoecol. 91, 291–304. http://dx.doi.org/10.1016/0031-0182(92)90073-E.
Meschede, M.A., Myhrvold, C.L., Tromp, J., 2011. Antipodal focusing of seismic waves due to large meteorite impacts on Earth. Geophys. J. Int. 187, 529–537. http://dx.doi.org/10.1111/j.1365-246X.2011.05170.x.
Mussard, M., Le Hir, G., Fluteau, F., Lefebvre, V., Goddéris, Y., 2014. Modeling the carbon–sulfate interplays in climate changes related to the emplacement of continental flood basalts. In: Keller, G., Kerr, A.C. (Eds.), Volcanism, Impacts, and Mass Extinctions: Causes and Effects. Geological Society of America Special Paper 505, pp. 339–352. http://dx.doi.org/10.1130/2014.2505(17).
Nordt, L., Atchley, S., Dworkin, S., 2003. Terrestrial evidence for two greenhouse events in the Latest Cretaceous. GSA Today 13, 4–9.
Olsson, R., Wright, J., Miller, K., 2001. Paleobiogeography of *Pseudotextularia elegans* during the latest Maastrichtian global warming event. J. Foraminifer. Res. 31, 275–282. http://dx.doi.org/10.2113/31.3.275.
Pardo, A., Keller, G., 2008. Biotic effects of environmental catastrophes at the end of the Cretaceous: *Guembelitria* and *Heterohelix* blooms. Cretac. Res. 29, 1058–1073. http://dx.doi.org/10.1016/j.cretres.2008.05.031.
Pardo, A., Ortiz, N., Keller, G., 1996. Latest Maastrichtian and Cretaceous–Tertiary boundary foraminiferal turnover and environmental changes at Agost, Spain. In: MacLeod, N., Keller, G. (Eds.), Cretaceous–Tertiary Boundary Mass Extinction: Biotic and Environmental Changes. Norton Press, New York, pp. 139–171.
Pringle, M.S., Frey, F.A., Mervine, E.M., 2008. A simple linear age progression for the Ninetyeast Ridge, Indian Ocean: new constraints on Indian plate tectonics and hotspot dynamics. Eos Transactions AGU Fall Meeting Supplementary Abstract 89, p. T54B-03.
Punekar, J., Mateo, P., Keller, G., 2014a. Environmental and biological effects of Deccan volcanism: a global survey. In: Keller, G., Kerr, A.C. (Eds.), Volcanism, Impacts, and Mass Extinctions: Causes and Effects. Geological Society of America Special Paper 505, p. SPE505-04. http://dx.doi.org/10.1130/2014.2505(04).
Punekar, J., Keller, G., Khozyem, H.M., Hamming, C., Adatte, T., Tantawy, A.A., Spangenberg, J., 2014b. Late Maastrichtian–early Danian high-stress environments and delayed recovery linked to Deccan volcanism. Cretac. Res. 49, 63–82. http://dx.doi.org/10.1016/j.cretres.2014.01.002.
Quillévéré, F., Norris, R.D., Kroon, D., Wilson, P.A., 2008. Transient ocean warming and shifts in carbon reservoirs during the early Danian. Earth Planet. Sci. Lett. 265, 600–615. http://dx.doi.org/10.1016/j.epsl.2007.10.040.
Renne, P.R., Deino, A.L., Hilgen, F.J., Kuiper, K.F., Mark, D.F., Mitchell III, W.S., Morgan, L.E., Mundil, R., Smit, J., 2013. Time scales of critical events around the Cretaceous–Paleogene boundary. Science 339, 684–687. http://dx.doi.org/10.1126/science.1230492.
Richards, M., Alvarez, W., Self, S., Karlstrom, L., Renne, P., Manga, M., Sprain, C., Smit, J., Vanderkluysen, L., Gibson, S.A., 2015. Triggering of the largest Deccan eruptions by the Chicxulub impact. Geol. Soc. Am. Bull. http://dx.doi.org/10.1130/B31167.1.
Robinson, N., Ravizza, G., Coccioni, R., Peucker-Ehrenbrink, B., Norris, R., 2009. A high resolution marine $^{187}Os/^{188}Os$ record for the late Maastrichtian: distinguishing the chemical fingerprints of Deccan volcanism and the KP impact event. Earth Planet. Sci. Lett. 281, 159–168. http://dx.doi.org/10.1016/j.epsl.2009.02.019.
Royer, J.-Y., Peirce, J.W., Weissel, J.K., 1991. Tectonic constraints on the hot-spot formation of Ninetyeast Ridge. Proc. Ocean Drill. Program 121, 763–776. http://dx.doi.org/10.2973/odp.proc.sr.121.122.1991.
Said, R., 1962. The Geology of Egypt. Elsevier, Amsterdam (377 pp.).
Schöbel, S., de Walla, H., Ganerødb, M., Panditc, M.K., Rolf, C., 2014. Magnetostratigraphy and $^{40}Ar–^{39}Ar$ geochronology of the Malwa Plateau region (Northern Deccan Traps), central western India: significance and correlation with the main Deccan Large Igneous Province sequences. J. Asian Earth Sci. 89, 28–45.
Schoene, B., Samperton, K.M., Eddy, M.P., Keller, G., Adatte, T., Bowring, S.A., Khadri, S.F.R., Gertsch, B., 2015. U–Pb geochronology of the Deccan Traps and relation to the end-Cretaceous mass extinction. Science 347, 182–184. http://dx.doi.org/10.1126/science.aaa0118.
Schulte, P., Alegret, L., Arenillas, I., Arz, J.A., Barton, P.J., Bown, P.R., Bralower, T.J., Christeson, G.L., Claeys, P., Cockell, C.S., Collins, G.S., Deutsch, A., Goldin, T.J., Goto, K., Grajales-Nishimura, J.M., Grieve, R.A.F., Gulick, S.P.S., Johnson, K.R., Kiessling, W., Koeberl, C., Kring, D.A., MacLeod, K.G., Matsui, T., Melosh, J., Montanari, A., Morgan, J.V., Neal, C.R., Nichols, D.J., Norris, R.D., Pierazzo, E., Ravizza, G., Rebolledo-Vieyra, M., Reimold, W.U., Robin, E., Salge, T., Speijer, R.P., Sweet, A.R., Urrutia-Fucugauchi, J., Vajda, V., Whalen, M.T., Willumsen, P.S., 2010. The Chicxulub asteroid impact and mass extinction at the Cretaceous–Paleogene boundary. Science 327, 1214–1218. http://dx.doi.org/10.1126/science.1177265.
Scotese, C.R., 2013. Map Folio 16, KT Boundary (65.5 Ma, latest Maastrichtian), PALEOMAP PaleoAtlas for ArcGIS, volume 2, Cretaceous, PALEOMAP Project, Evanston, IL.
Self, S., Jay, A.E., Widdowson, M., Keszthelyi, L.P., 2008. Correlation of the Deccan and Rajahmundry Trap lavas: are these the longest and largest lava flows on Earth? J. Volcanol. Geotherm. Res. 172, 3–19. http://dx.doi.org/10.1016/j.jvolgeores.2006.11.012.
Sheldon, E., Ineson, J., Bown, P., 2010. Late Maastrichtian warming in the Boreal Realm: Calcareous nannofossil evidence from Denmark. Palaeogeogr. Palaeoclimatol. Palaeoecol. 295, 55–75. http://dx.doi.org/10.1016/j.palaeo.2010.05.016.
Stüben, D., Kramar, U., Berner, Z.A., Meudt, M., Keller, G., Abramovich, S., Adatte, T., Hambach, U., Stinnesbeck, W., 2003. Late Maastrichtian paleoclimatic and paleoceanographic changes inferred from Sr/Ca ratio and stable isotopes. Palaeogeogr. Palaeoclimatol. Palaeoecol. 199, 107–127. http://dx.doi.org/10.1016/S0031-0182(03)00499-1.
Stüben, D., Kramar, U., Harting, M., Stinnesbeck, W., Keller, G., 2005. High-resolution geochemical record of Cretaceous–Tertiary boundary sections in Mexico: new constraints on the K/T and Chicxulub events. Geochim. Cosmochim. Acta 69, 2559–2579. http://dx.doi.org/10.1016/j.gca.2004.11.003.
Tantawy, A.A., Keller, G., Adatte, T., Stinnesbeck, W., Kassab, A., Schulte, P., 2001. Maastrichtian to Paleocene (Dakhla Formation) depositional environment of the Western Desert in Egypt: sedimentology, mineralogy and integrated micro- and macrofossil biostratigraphies. Cretac. Res. 22, 795–827. http://dx.doi.org/10.1006/cres.2001.0291.
Tantawy, A.A., Keller, G., Pardo, A., 2009. Late Maastrichtian volcanism in the Indian Ocean: effects on calcareous nannofossils and planktic foraminifera. Palaeogeogr. Palaeoclimatol. Palaeoecol. 284, 63–87. http://dx.doi.org/10.1016/j.palaeo.2009.08.025.
Thibault, N., Gardin, S., 2006. Maastrichtian calcareous nannofossil biostratigraphy and paleoecology in the Equatorial Atlantic (Demerara Rise, ODP Leg 207 Hole 1258A). Rev. Micropaleontol. 49, 199–214. http://dx.doi.org/10.1016/j.revmic.2006.08.002.
Thibault, N., Gardin, S., 2007. The late Maastrichtian nannofossil record of climate change in the South Atlantic DSDP Hole 525A. Mar. Micropaleontol. 65, 163–184. http://dx.doi.org/10.1016/j.marmicro.2007.07.004.
Thibault, N., Gardin, S., 2010. The calcareous nannofossil response to the end-Cretaceous warm event in the Tropical Pacific. Palaeogeogr. Palaeoclimatol. Palaeoecol. 291, 239–252. http://dx.doi.org/10.1016/j.palaeo.2010.02.036.
Thibault, N., Husson, D., 2016. Climatic fluctuations and sea surface water circulation patterns at the end of the Cretaceous era: calcareous nannofossil evidence. Palaeogeogr. Palaeoclimatol. Palaeoecol. Spec. Issue 441, 152–164 (in this issue).
Thibault, N., Galbrun, B., Gardin, S., Minoletti, F., Le Callonec, L., 2015a. The end-Cretaceous in the southwestern Tethys (Elles, Tunisia): orbital calibration of paleoenvironmental events before the mass extinction. Int. J. Earth Sci. 1–25 http://dx.doi.org/10.1007/s00531-015-1192-0.
Thibault, N., Anderskouv, K., Bjerager, M., Boldreel, L.O., Jelby, M.E., Stemmerik, L., Surlyk, F., 2015b. Upper Campanian–Maastrichtian chronostratigraphy of the Skaelskor-1 core, Denmark: correlation at the basinal and global scale and implications for changes in sea-surface temperatures. Lethaia http://dx.doi.org/10.1111/let.12128.
Wilf, P., Johnson, K.R., Huber, B.T., 2003. Correlated terrestrial and marine evidence for global climate changes before mass extinction at the Cretaceous–Paleogene boundary. Proc. Natl. Acad. Sci. U. S. A. 100, 599–604. http://dx.doi.org/10.1073/pnas.0234701100.